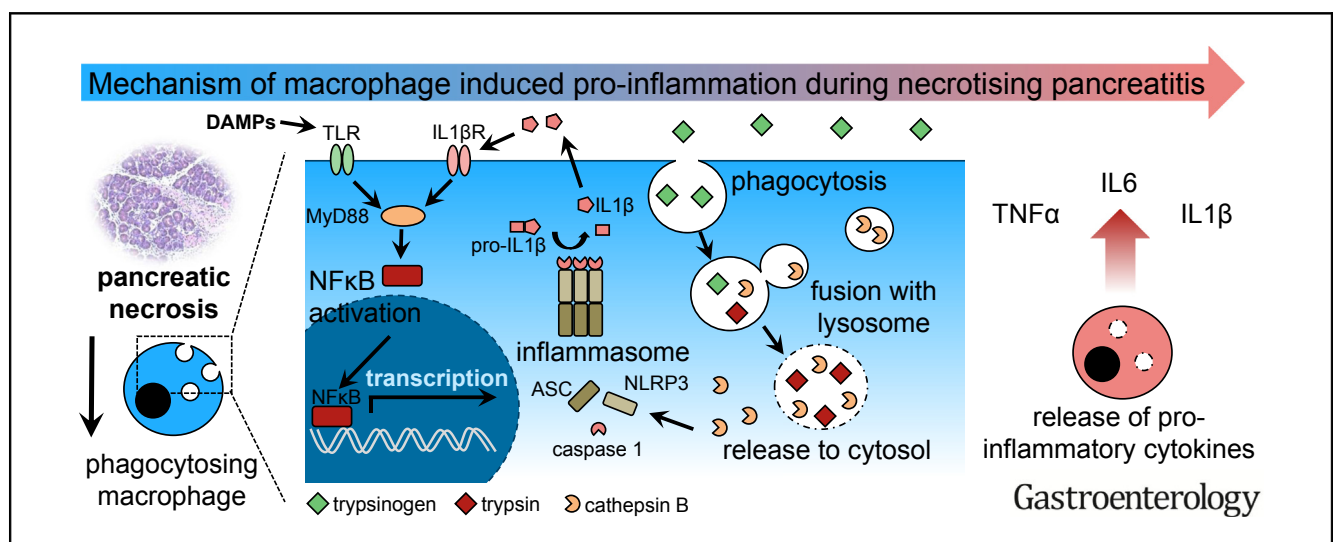




# Cathepsin B-Mediated Activation of Trypsinogen in Endocytosing Macrophages Increases Severity of Pancreatitis in Mice

Matthias Sendler,<sup>1</sup> Frank-Ulrich Weiss,<sup>1</sup> Janine Golchert,<sup>2</sup> Georg Homuth,<sup>2</sup> Cindy van den Brandt,<sup>1</sup> Ujjwal M. Mahajan,<sup>6</sup> Lars-Ivo Partecke,<sup>3</sup> Paula Döring,<sup>4</sup> Ilya Gukovsky,<sup>5</sup> Anna S. Gukovskaya,<sup>5</sup> Preshit R. Wagh,<sup>1</sup> Markus M. Lerch,<sup>1,§</sup> and Julia Mayerle<sup>1,6,§</sup>

<sup>1</sup>Department of Medicine A, University Medicine Greifswald, Greifswald, Germany; <sup>2</sup>Interfaculty Institute for Genetics and Functional Genomics, University Medicine Greifswald, Greifswald, Germany; <sup>3</sup>Department of Surgery, University Medicine Greifswald, Greifswald, Germany; <sup>4</sup>Institute of Pathology, University Medicine Greifswald, Greifswald, Germany; <sup>5</sup>VA Greater Los Angeles Healthcare System; David Geffen School of Medicine, University of California at Los Angeles, California; and <sup>6</sup>Medizinische Klinik und Poliklinik II, Universitätsklinikum der Ludwig-Maximilians-Universität, Klinikum Grosshadern, Munich, Germany



See editorial on page 482.

**BACKGROUND & AIMS:** Acute pancreatitis is characterized by premature intracellular activation of digestive proteases within pancreatic acini and a consecutive systemic inflammatory response. We investigated how these processes interact during severe pancreatitis in mice. **METHODS:** Pancreatitis was induced in C57Bl/6 wild-type (control), cathepsin B (CTSB)-knockout, and cathepsin L-knockout mice by partial pancreatic duct ligation with supramaximal caerulein injection, or by repetitive supramaximal caerulein injections alone. Immune cells that infiltrated the pancreas were characterized by immunofluorescence detection of Ly6g, CD206, and CD68. Macrophages were isolated from bone marrow and incubated with bovine trypsinogen or isolated acinar cells; the macrophages were then transferred into pancreatitis control or cathepsin-knockout mice. Activities of proteases and nuclear factor (NF)-κB were determined using fluorogenic substrates and trypsin activity was blocked by nafamostat. Cytokine levels were measured using a cytometric bead array. We performed immunohistochemical analyses to detect

trypsinogen, CD206, and CD68 in human chronic pancreatitis (n = 13) and acute necrotizing pancreatitis (n = 15) specimens. **RESULTS:** Macrophages were the predominant immune cell population that migrated into the pancreas during induction of pancreatitis in control mice. CD68-positive macrophages were found to phagocytose acinar cell components, including zymogen-containing vesicles, in pancreata from mice with pancreatitis, as well as human necrotic pancreatic tissues. Trypsinogen became activated in macrophages cultured with purified trypsinogen or co-cultured with pancreatic acini and in pancreata of mice with pancreatitis; trypsinogen activation required macrophage endocytosis and expression and activity of CTSB, and was sensitive to pH. Activation of trypsinogen in macrophages resulted in translocation of NF-κB and production of inflammatory cytokines; mice without trypsinogen activation (CTSB-knockout mice) in macrophages developed less severe pancreatitis compared with control mice. Transfer of macrophage from control mice to CTSB-knockout mice increased the severity of pancreatitis. Inhibition of trypsin activity in macrophages prevented translocation of NF-κB and production of inflammatory cytokines. **CONCLUSIONS:** Studying pancreatitis in mice, we found

## EDITOR'S NOTES

## BACKGROUND AND CONTEXT

Necrotizing acute pancreatitis induces an overwhelming systemic inflammatory response (SIRS), which is mediated by infiltrating phagocytosing macrophages. Persistent SIRS results in multiorgan failure.

## NEW FINDINGS

Pancreatic protease activation, a hallmark of acute pancreatitis, is not restricted to acinar cells but phagocytosing macrophages are able to intracellularly activate trypsinogen to trypsin in a cathepsin B dependent manner. Active trypsin inside macrophages acts as DAMP and fuels systemic inflammation.

## LIMITATIONS

Macrophage mediated protease activation is limited to a severe model of acute necrotising pancreatitis.

## IMPACT

Intrapancreatic protease activation within macrophages is directly linked to NF $\kappa$ B activation and the systemic inflammatory response determining severity of the disease. This allows therapeutic targeting of two causal mechanisms in pancreatitis.

activation of digestive proteases to occur not only in acinar cells but also in macrophages that infiltrate pancreatic tissue. Activation of the proteases in macrophage occurs during endocytosis of zymogen-containing vesicles, and depends on pH and CTSB. This process involves macrophage activation via NF- $\kappa$ B-translocation, and contributes to systemic inflammation and severity of pancreatitis.

**Keywords:** Pancreatic Inflammation; Mechanisms; Immune Response; Mouse Model.

Acute pancreatitis is common and of increasing incidence in Western countries.<sup>1</sup> The majority of cases suffer from a mild form of the disease but approximately 20% of patients develop severe pancreatitis, associated with pancreatic necrosis, systemic inflammation, and organ failure.<sup>2</sup> An overwhelming systemic immune reaction, the so-called systemic inflammatory response syndrome, accounts for persistent multiorgan failure and seems to be responsible for the majority of systemic complications and mortality.<sup>3</sup> The triggering events of this immune reaction and the pathophysiological mechanism that determine severity of the disease are still poorly understood.<sup>4</sup>

Self-digestion by its own proteases is considered to be a trigger of pancreatitis. Under pathologic conditions, the digestive serine protease trypsinogen is converted to active trypsin by the lysosomal hydrolase cathepsin B (CTSB) within the acinar cells.<sup>5-7</sup> Premature intracellular protease activation is then followed by acinar cell death, which is accompanied by a pro-inflammatory response and leads to a prominent translocation of leukocytes. Especially cells of the innate immune system migrate into the injured organ.<sup>8</sup> These cells are the first cells that reach the

pancreas.<sup>9,10</sup> This immune reaction boosts local damage and results in an increase in severity of disease.<sup>10,11</sup> The importance of the protease/anti-protease balance for the development of pancreatitis is supported by the observation that germline mutations that increase the susceptibility toward developing pancreatitis mostly affect genes of the protease/anti-protease system, such as cationic-trypsinogen (PRSS1), chymotrypsin-C (CTRC) or the trypsin-inhibitor SPINK1.<sup>12-16</sup> How the intracellular activation of digestive proteases is linked to local and systemic inflammatory reaction is still being debated. On the one hand, acinar cells under experimental conditions activate nuclear factor  $\kappa$ B,<sup>17</sup> a key transcription factor for the pro-inflammatory response, but still do so in animals in which T7-trypsinogen, a major mouse-isoform of trypsinogen, has been deleted.<sup>18</sup> On the other hand, acinar cell that undergo autodigestion and necrosis release damage-associated molecular patterns (DAMPs) such as free DNA, histones, or free adenosine triphosphate (ATP), which are recognized by immune cell receptors inducing a pro-inflammatory reaction and activation of the inflammasome pathway.<sup>19</sup> The main task of infiltrating immune cells in the pancreas is thought to be defensive and includes the removal of cellular debris and necrosis. Most of the clearance is achieved through the action of macrophages that not only phagocytose cellular debris,<sup>20</sup> but whose involvement in the subsequent immune reaction is profoundly influenced by what cellular components they are exposed to and which ones they ingest.<sup>21</sup> For example, their clearance of apoptotic cellular waste involves largely non-inflammatory pathways whereby components of necrotic cells can trigger a pro-inflammatory response.<sup>21</sup> In the present study we found that, in areas of pancreatic necrosis, macrophages ingest zymogen-containing vesicles from damaged acinar cells that they convert these zymogens to active proteases in a CTSB-dependent manner and that the intramacrophage activation of trypsinogen is an important driver of local and systemic inflammation and disease severity.

## Material and Methods

### Isolation of Pancreatic Acini

Acini were isolated from mouse pancreas by collagenase digestion under sterile conditions, as previously reported.<sup>6</sup> For details see [Supplementary Materials and Methods](#).

<sup>§</sup> Authors share co-senior authorship.

**Abbreviations used in this paper:** ATP, adenosine triphosphate; BMDM, bone marrow-derived macrophages; CCK, cholecystokinin; CTSB, cathepsin B; CTSL, cathepsin L; DAMP, damage-associated molecular pattern; IL, interleukin; LPS, lipopolysaccharide; MCP-1, monocyte chemoattractant protein-1; NK $\kappa$ Bp65, nuclear factor  $\kappa$ B p65; NLRP3, nucleotide-binding oligomerization domain-like receptor family pyrin domain-containing 3; TNF $\alpha$ , tumor necrosis factor  $\alpha$ ; WT, wild-type.

 Most current article

© 2018 by the AGA Institute. Published by Elsevier Inc. This is an open access article under the CC BY-NC-ND license (<http://creativecommons.org/licenses/by-nc-nd/4.0/>).

0016-5085

<https://doi.org/10.1053/j.gastro.2017.10.018>

### Isolation of Bone Marrow-derived Macrophages

Bone marrow-derived macrophages (BMDM) were isolated from the femur and tibia of mice. A detailed protocol is provided in the [Supplementary Materials](#).

### Biochemical Assays

Serum amylase and different protease activities were measured as previously reported using substrates R110-Ile-Pro-Arg for trypsin, Suc-Ala-Ala-Pro-Phe-AMC for chymotrypsin, R110-Phe-Arg for CTSL, and AMC-Arg<sub>2</sub> for CTBS.<sup>22</sup> For details on in vivo imaging of proteases see [Supplementary Materials](#).

### Induction of Pancreatitis in Mice

All animal experiments were performed after prior approval by the Institutional Animal Care committee. C57Bl/6 mice were obtained from Charles River (Sulzfeld, Germany), CTBS<sup>-/-</sup>, cathepsin L (CTSL)<sup>-/-</sup>, and nucleotide-binding oligomerization domain-like receptor family pyrin domain-containing 3 (NLRP3)<sup>-/-</sup> mice were maintained in our animal facility; all mice strains are bred with a C57Bl/6 background.

### Histology, Immunohistochemistry, and Immunofluorescence

Paraffin sections were used for H&E staining and Masson-Goldner-trichrome staining as previously reported.<sup>23</sup> For details see [Supplementary Materials](#).

### Human Pancreatic Samples

Human chronic pancreatitis tissue was collected in the context of the ChroPac trial (ISRCTN38973832; <http://www.isrctn.com/ISRCTN38973832>).<sup>24</sup> Necrotic tissue was harvested during endoscopic necrosectomy under the ethics committee approval for the ProZyt trial.

### Statistical Analysis

All data are expressed as means ± standard error of the mean from at least 5 animals or experiments. Statistical analysis was performed using SigmaPlot and SigmaStat. Unpaired 2-tailed Student's *t*-test or Rank-Sum test were used. Differences were considered significant for  $P < .05$ .

## Results

### Migration of Macrophages in Acute Pancreatitis

To study the pancreatic infiltrate we used 2 different models of acute pancreatitis: caerulein-induced pancreatitis and partial duct ligation to study extensive necrosis and exocrine tissue replacement by fibrosis after 14 days, as shown by H&E staining ([Figure 1A](#)).<sup>23</sup>

Staining of Ly6g illustrates the infiltration of granulocytes in pancreatic tissue. CD68 and CD206 are markers for macrophages, whereas CD68 is an indicator of the pro-inflammatory M1-phenotype and CD206 is only expressed on alternatively activated M2 macrophages. In contrast to the mild model of pancreatitis, the infiltration in severe necrotizing pancreatitis was dominated by CD68-positive

macrophages ([Figure 1A](#)). Quantification of infiltrating cells per microscopic field revealed that CD68-positive macrophages represented the majority of infiltrating leukocytes in the ligation model of pancreatitis ([Figure 1B](#)), corresponding with the severity of the model. The number of infiltrating Ly6g-positive granulocytes did not differ between the pancreatitis models ([Figure 1B](#)). [Supplementary Figure 1A](#) and [1B](#) show representative examples for the necrosis/fibrosis sequence in the ligation pancreatitis model. Alternatively, activated M2 macrophages were found increased at later time points (7 days and 14 days after duct ligation), which corresponded to the development of fibrosis. Whereas the number of M1 macrophages corresponded to the extent of necrosis at earlier time points ([Figure 1B](#) and [1C](#)). Not only the number and phenotype of macrophages but also their morphology differed between models and over time ([Figure 1D](#)). Especially in necrotic areas, the size of infiltrating cells was significantly increased ([Figure 1D](#)).

It is well established that macrophages are responsible for clearance of necrotic areas by phagocytosing cellular debris.<sup>20</sup> Co-labeling for trypsinogen, which is exclusively expressed by acinar cells, and CD68 suggested that macrophages phagocytose pancreatic enzymes or enzyme-containing vesicles from injured acinar cells within necrotic areas ([Figure 1E](#)). This phenomenon could only be observed in macrophages, where punctate vesicles contained trypsinogen, but not in other inflammatory cells ([Figure 1F](#)). Co-localization with chymotrypsin, another pancreatic serine-protease, was found in CD68-positive cells ([Supplementary Figure 1C](#)). CD68 positive M1 macrophages are mainly detected within necrotic areas, whereas CD206-positive cells are found in non-necrotic parts of the pancreas. Interestingly, we did not detect co-localization of trypsinogen within CD206-positive cells even 14 days post-ligation. Only few CD68-positive cells stained positive for trypsinogen later in the disease course ([Supplementary Figure 1D-F](#)). These data indicate that M1 macrophages in necrotic tissue areas of the pancreas ingest zymogen-containing components of acinar cells.

### Macrophages Phagocytosing Digestive Zymogens From Injured Acinar Cells Undergo Activation

To investigate the role of phagocytosing macrophages, we performed co-incubation experiments using bone marrow-derived macrophages and freshly prepared acinar cells. Pure macrophages in culture are shown in [Figure 2A](#). Isolated acini were stimulated with 1 μmol/L cholecystokinin (CCK) before co-incubation. Staining of trypsinogen and CD68 allowed discrimination between acinar cells and macrophages ([Figure 2A](#)) and showed that macrophages co-localize with zymogens or zymogen-containing vesicles from damaged acinar cells in vitro.

Staining macrophages for nuclear factor κB p65 (NFκBp65) revealed a cytoplasmic distribution in unstimulated control cells, whereas 6 hours of co-incubation



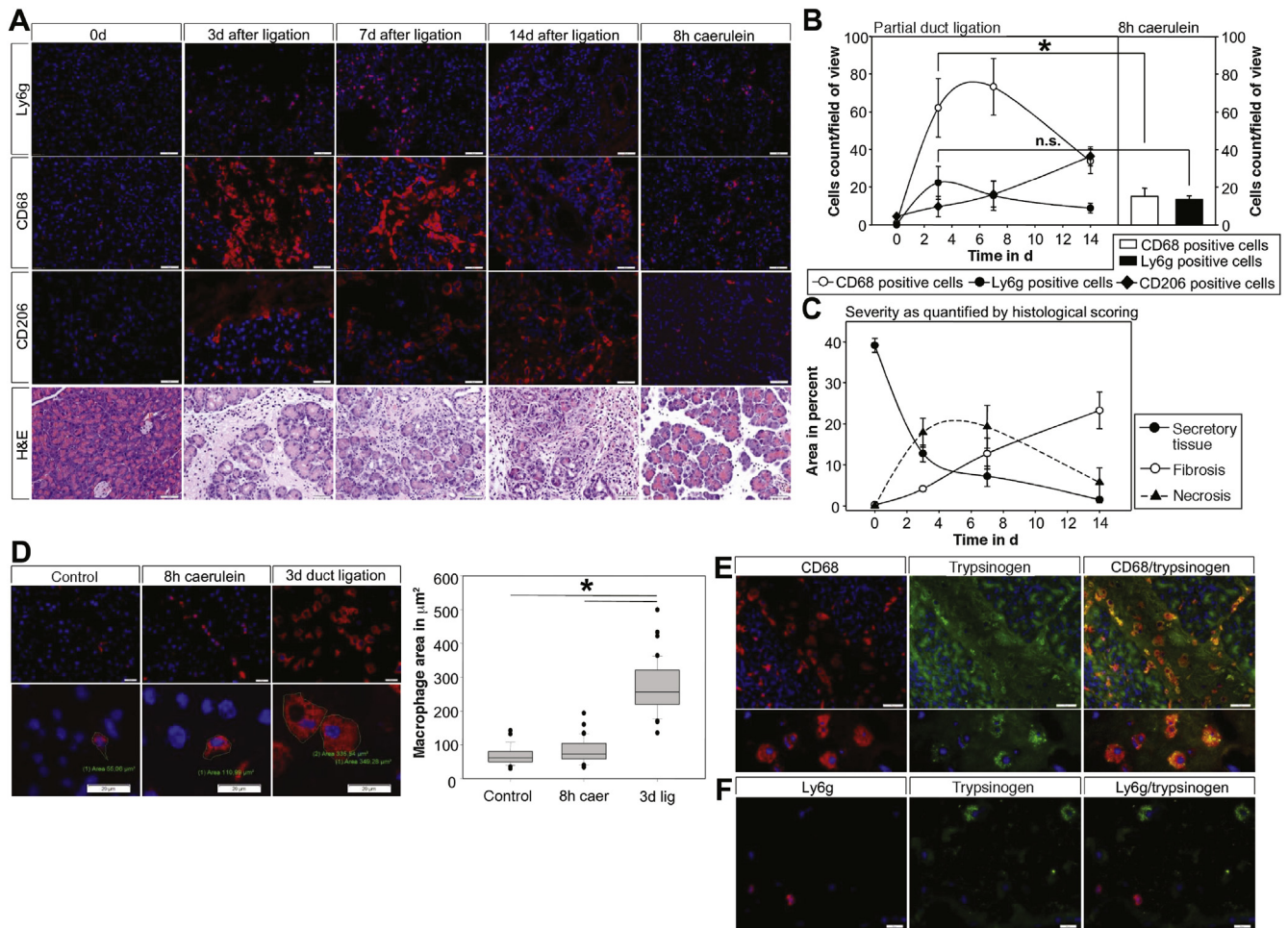


**Figure 1.** Severe acute pancreatitis was induced by duct ligation and supramaximal caerulein stimulation. Infiltrating immune cells of the innate immune system were stained in pancreatic tissue (A) and quantified by cell counting (B). Time course and amount of neutrophil infiltration (Ly6g) and M1 macrophage (CD68) infiltration in the severe model of acute pancreatitis was compared with the mild form of the disease. H&E staining of the pancreas illustrating the severity of disease. The inflammatory infiltrate correlates with the amount of necrotic areas and the decrease of unaffected healthy exocrine tissue (C). The number of M2 macrophages (CD206) rises with increasing fibrosis (C). Three days after duct ligation the shape and volume of macrophages is significantly altered and increased in CD68-positive macrophages (D). Large CD68-positive macrophages display co-localization with pancreatic trypsinogen (E), indicating phagocytosis of dying acini or cellular waste. Neutrophils did not show any co-localization with trypsinogen (F). Asterisks (\*) indicate significant differences with  $P < .05$  ( $n = 5-8$ ).

with CCK-stimulated acini induced a translocation of  $\text{NF}\kappa\text{Bp}65$  into the nucleus of CD68-positive macrophages (Figure 2B). In the same setting, co-incubation of macrophages with CCK-stimulated acini resulted in a significant increase of cytokine secretion, here shown for the pro-inflammatory cytokines interleukin-6 (IL6) and tumor necrosis factor  $\alpha$  ( $\text{TNF}\alpha$ ), as well as the chemokine monocyte chemoattractant protein-1 (MCP-1) (Figure 2C). Lipopolysaccharide (LPS)-stimulated macrophages served as controls. Acini were also able to secrete cytokines, but the majority of cytokine release originated from macrophages (Figure 2C). When morphology of macrophages was analyzed for cell size (Figure 2D), co-incubation with acini in vitro resulted in a significant change in macrophage morphology, resembling the results of tissue sections (Figure 1D). Macrophages developed a spreading phenotype and changed their morphology in forward side scatter on

fluorescence-activated cell sorter analysis (Figure 2E). Macrophages are activated upon co-incubation with acini or isolated zymogen granules (Figure 2F), which are engulfed by macrophages (Supplementary Figure 2A-C). These data indicate that co-incubation of macrophages with acinar cells results in activation of macrophages and a differentiation to a pro-inflammatory M1 phenotype.

*Macrophages Phagocytose Zymogen-containing Vesicles and Activate Trypsinogen Intracellularly in a CTSB-dependent Manner*

The detection of trypsin activity within phagocytosing macrophages raised the question whether activated trypsin was engulfed or whether macrophages activate trypsinogen intracellularly. We therefore isolated macrophages from bone marrow of C57Bl/6 mice and co-incubated them with



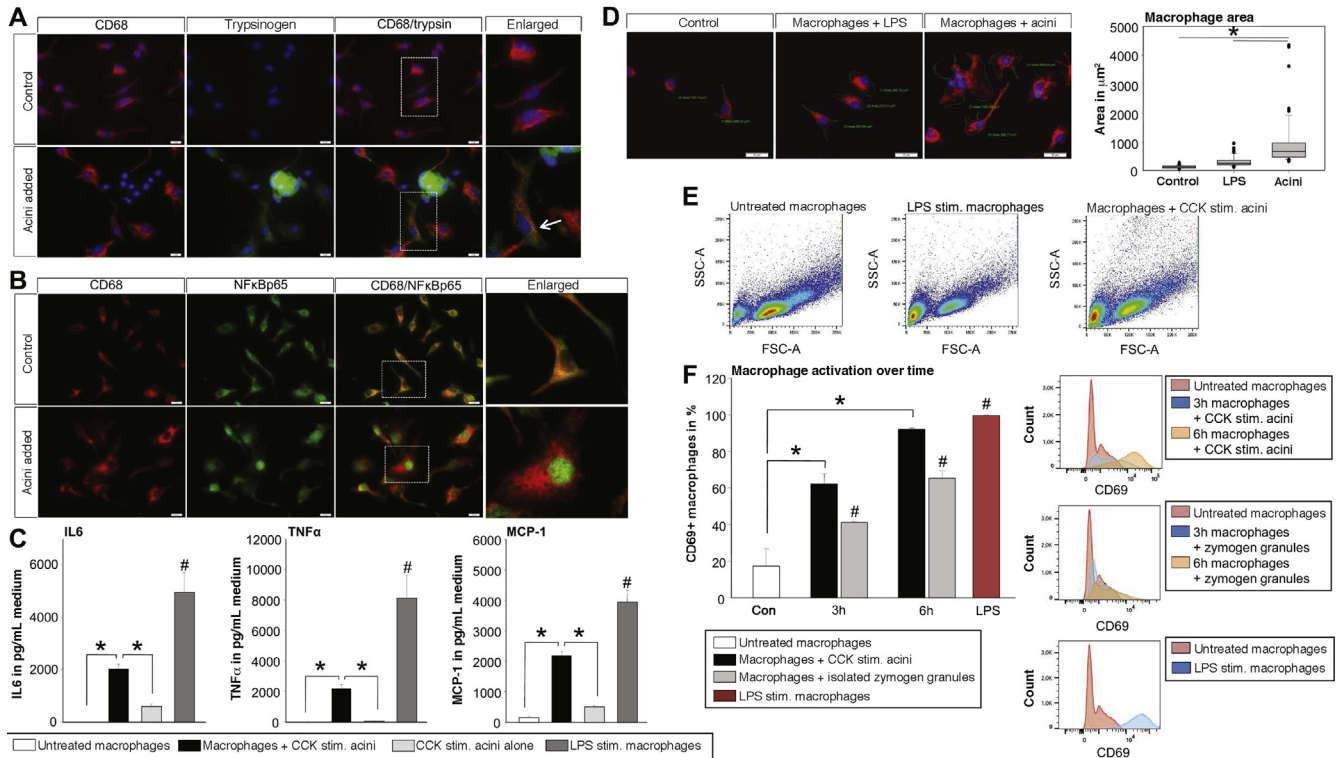


**Figure 2.** BMDM were co-incubated with CCK-stimulated acini. Staining of CD68 marked macrophages, whereas trypsinogen was used as a marker for acini (A). Phagocytosis of acinar cell compartments is demonstrated by intra-macrophage trypsinogen staining (arrow). Six hours after co-incubation the transcription factor NF $\kappa$ Bp65 showed nuclear translocation in macrophages compared with untreated controls (B). Cytokine secretion of macrophages was significantly increased after 6 hours of co-incubation, as seen by secretion IL6, TNF $\alpha$ , and MCP-1. Acini alone showed a significantly lower secretion of these cytokines (C). Treatment of macrophages with LPS served as control. Furthermore, macrophage morphology changed during co-incubation (D-E). CD69, an early activation marker belonging to the C-type lectin domain family, is increased on macrophages co-incubated with acini or isolated zymogen granules (F). Asterisks (\*) indicate significant differences with  $P < .05$  ( $n = 6$ ); # indicate a significant difference to all other conditions.

bovine trypsinogen in a concentration of 10  $\mu$ g/mL (see [Supplementary Figure 2D](#)). Labelling for trypsinogen and CD68 indicated that trypsinogen is internalized by macrophages ([Figure 3A](#)) and then converted to active trypsin intracellularly ([Figure 3B](#)). Intracellular trypsin activity in macrophages could be blocked completely by 50  $\mu$ mol/L nafamostat, a potent digestive serine protease inhibitor, by bafilomycin-A1, an inhibitor of V-ATPases that neutralizes the usually acidic intravesicular pH, and by CA074me, a cell permeant CTSB inhibitor. Both substances led to a pronounced reduction in CTSB and trypsin activity in macrophages ([Figure 3B](#)). Furthermore, in vivo imaging of isolated macrophages co-incubated with trypsinogen revealed active trypsin inside macrophages ([Figure 3C](#)). Final evidence that trypsinogen undergoes activation in a CTSB-dependent manner within phagocytosing macrophages came from experiments using CTSB- and CTSL-deleted mouse macrophages incubated with bovine trypsinogen. Trypsin activity was significantly reduced in macrophages from CTSB $^{-/-}$  mice while it was increased in macrophages from CTSL $^{-/-}$  mice ([Figure 3D](#)), which is in accordance with the counteracting role of CTSL to CTSB.<sup>25</sup> Immunofluorescence staining for CTSB and trypsinogen in macrophages incubated with bovine trypsinogen revealed a punctate

localization of both enzymes in a vesicular compartment of macrophages ([Figure 3E](#)). These experiments show that macrophages activate phagocytosed trypsinogen intracellularly.

Co-incubation of BMDM with freshly prepared and CCK-stimulated acini (rather than trypsinogen) again resulted in intracellular localization of trypsinogen as well as amylase within macrophages. In addition, a co-localization of CTSB with trypsinogen was observed ([Figure 4A](#)). Intracellular localization of protease activity showed a membrane-confined punctate localization for active trypsin and active chymotrypsin ([Figure 4B](#)). Furthermore, fluorescent-labeled zymogen granules showed trypsin activity visualized by R110-Ile-Pro-Arg cleavage ([Supplementary Figure 2A](#)). Western blotting of macrophage lysates confirmed the intracellular presence of trypsinogen and amylase ([Figure 4C](#)). Activity of trypsin in macrophages after co-incubation with acini was significantly increased. Even when macrophages were co-incubated with acini isolated from CTSB $^{-/-}$  mice, we observed a significant increase in trypsin activity ([Figure 4D](#)), indicating that macrophage CTSB, rather than acinar cell CTSB, drives trypsin activation. When we used macrophages isolated from CTSB $^{-/-}$  mice we found no increase in trypsin activity after co-incubation

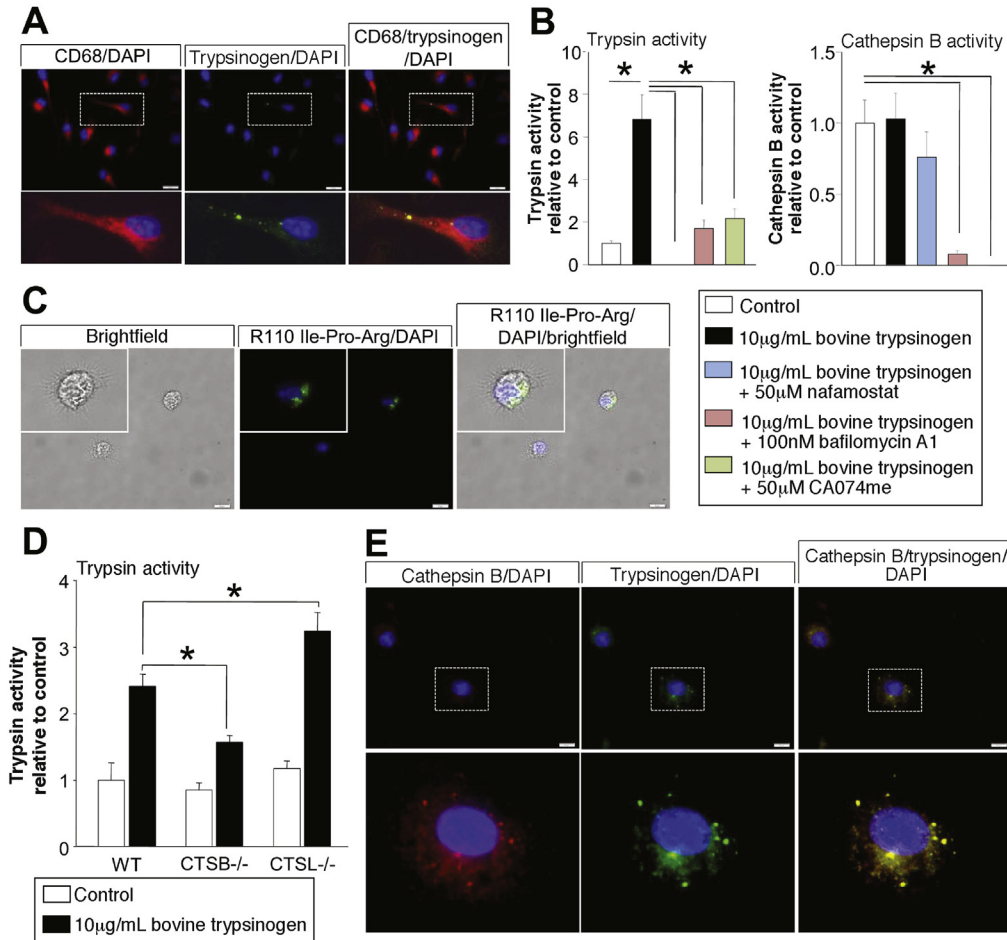


**Figure 3.** BMDM were co-incubated with bovine trypsinogen over a time period of 6 hours. Immunofluorescence staining of trypsinogen revealed an intracellular membrane confined punctiform localization within CD68-positive macrophages after 6 hours (A). Activity measurements in cell lysates of macrophages proved a significant increase of trypsin activity in macrophages co-incubated with trypsinogen. Nafamostate, CA074me, or bafilomycin-A1 and lysosomal acidification were able to completely block trypsin activity (B), but only CA074me and bafilomycin-A1 caused a significant decrease in CTBSB activity (B). Visual detection of active trypsin by the fluorogenic substrate R110-CBZ-Ile-Pro-Arg demonstrated intracellular located trypsin activity within macrophages (C). Comparison of WT macrophages with CTBSB or CTSL-deficient macrophages showed significantly decreased trypsin activity in CTBSB-deleted macrophages and increased activity in CTSL-deleted cells (D). Immunofluorescence staining indicates co-localization of phagocytosed trypsinogen and macrophage CTBSB (E). Asterisks (#) indicate significant differences with  $P < .05$  ( $n = 4-6$ ).

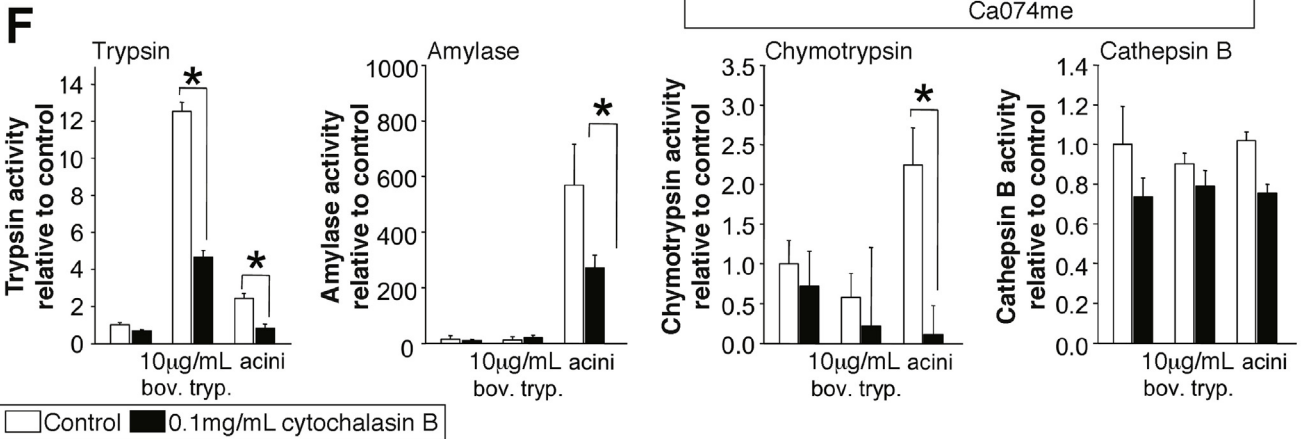
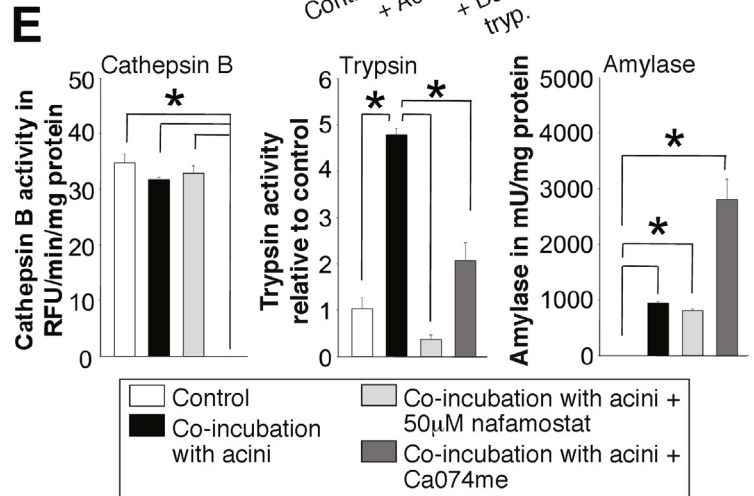
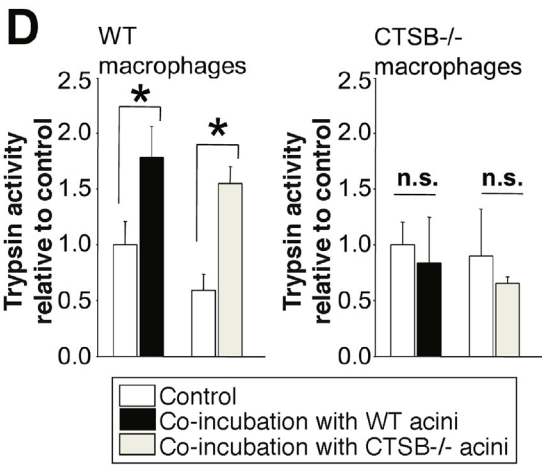
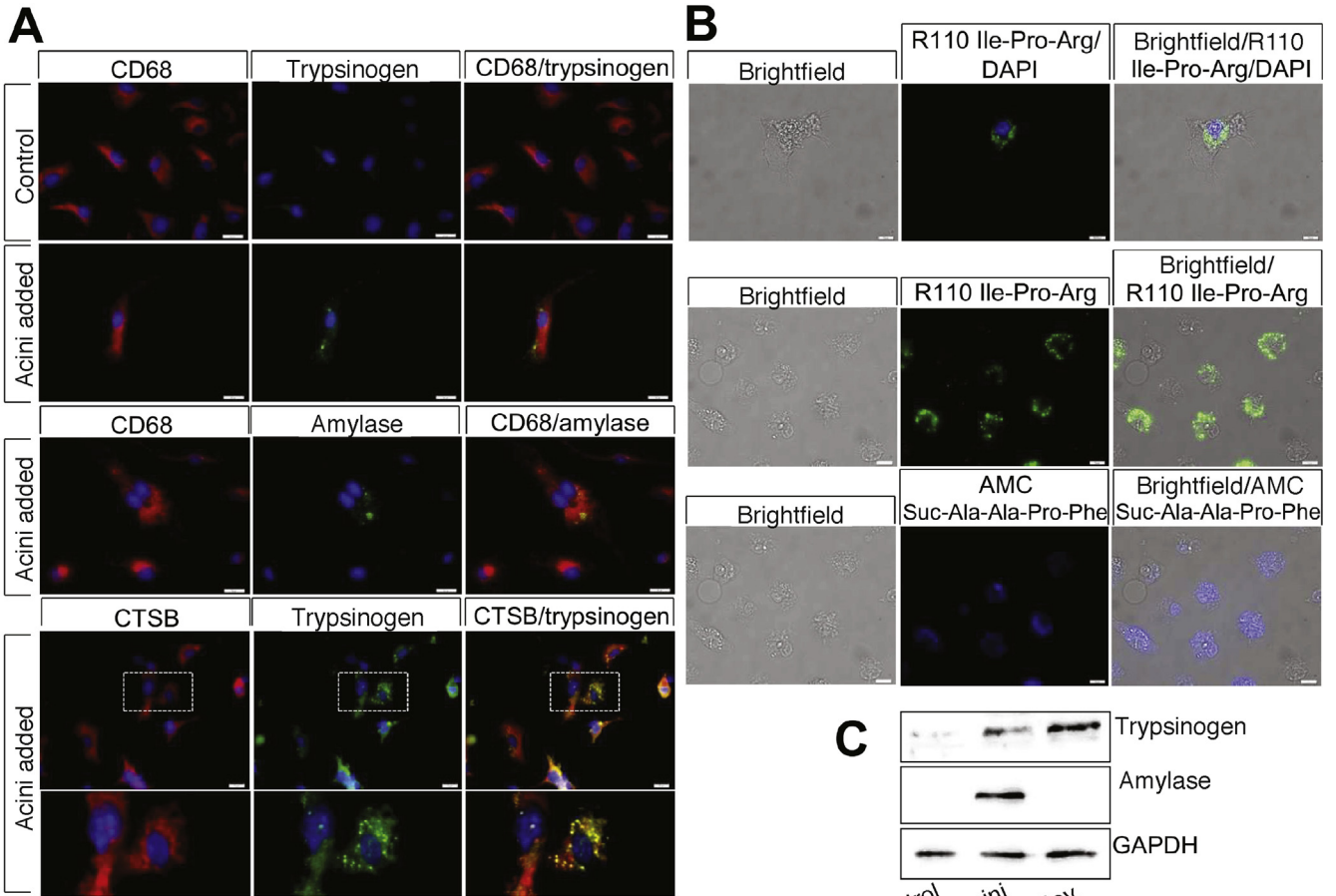
with acini from wild-type (WT) or CTBSB<sup>-/-</sup> mice. Both nafamostate and CA074me blocked trypsin activity after co-incubation (Figure 4E), indicating that intracellular trypsin activation in macrophages is entirely dependent on the presence and activity of CTBSB. Amylase activity was measured in macrophages as a marker of phagocytosis of acinar cell components. Uptake was not impaired by nafamostate pretreatment, whereas pretreatment of macrophages with CA074me resulted in an increase in intracellular amylase activity (Figure 4E), indicating that inhibition of CTBSB leads to impaired degradation of amylase. To investigate whether phagocytosis is the mechanism of uptake for pancreatic zymogens, we used cytochalasin-B to block phagocytosis by inhibition of the network formation of actin filaments.<sup>26</sup> Cytochalasin-B greatly reduced trypsin, chymotrypsin, and amylase activity in macrophages exposed to either bovine trypsinogen or acinar cells (Figure 4F). The

activity of CTBSB was not affected by cytochalasin-B treatment (Figure 4F).

**Blockade of Digestive Protease Activation Within Macrophages Reduces Pro-inflammatory Signaling and Cytokine Secretion**

Macrophages engulf cellular debris from injured acini and incorporate pancreatic zymogens and zymogen-containing vesicles. Phagocytosed zymogens, especially trypsinogen, undergo activation in a CTBSB-dependent manner within macrophages. We therefore investigated the effect of this intracellular protease activation on macrophages.

Translocation of NFκBp65 into the nucleus indicates pro-inflammatory differentiation of macrophages (M1). Co-incubation of BMDM with CCK-stimulated acini resulted





in a nuclear redistribution of NF $\kappa$ Bp65. This translocation was blocked by nafamostat (Figure 5A), indicating that trypsin activity is involved in this process. Untreated macrophages served as negative controls while LPS treatment served as positive controls (Figure 5A). Both nafamostat and bafilomycin-A1 abolished intracellular trypsin activity without affecting phagocytosis, as shown by an unimpaired amylase uptake (Figure 5B). Cytokine release of macrophages co-incubated with acini was determined by cytometric bead array. Treatment with nafamostat significantly reduced secretion of pro-inflammatory cytokines such as IL6, MCP-1, and TNF $\alpha$ . Treatment with bafilomycin-A1 had a similar effect, with the exception of TNF $\alpha$  (Figure 5C). The effect of bafilomycin-A1 on TNF $\alpha$  secretion in macrophages has been described previously.<sup>27</sup> Comparing the cytokine release of macrophages from WT mice with CTSB $^{-/-}$  cells, we found significantly reduced IL6, TNF $\alpha$ , and MCP-1 secretion after co-incubation with acini (Figure 5D). This is not a generalized defect because CTSB $^{-/-}$  macrophages responded to LPS adequately and in the same manner as WT macrophages (Supplementary Figure 2E). Transcriptome analysis of macrophages was performed 6 hours after co-incubation with acini. Transcriptional alteration of NF $\kappa$ B-related genes was affected by pre-treatment with nafamostat, blocking intracellular trypsin activity and proving a trypsin-mediated effect on NF $\kappa$ B-signaling. In particular, *Nfkb2* and *Rela* were significantly decreased (Student's *t*-test of fold change) (Figure 5E and 5F).

These data suggest that the pro-inflammatory phenotype of macrophages in pancreatitis is dependent on CTSB-mediated trypsinogen activation within phagocytosing macrophages.

### Protease Activation Within Macrophages Acts as DAMP and Induces NLRP3 Inflammasome Activation

Pathway analysis of macrophage transcriptome data by Ingenuity Pathway Analysis shows a significant down-regulation of the toll-like receptor pathways, as well as the NF $\kappa$ B pathway, after co-incubation with acini and trypsin inhibition by nafamostat (Figure 6A). MyD88 is the upstream regulator ( $P = 2.0E^{-6}$ ) that is affected most. Detailed analysis of the NF $\kappa$ B pathway suggests a critical role of IL1 $\beta$  for the activation of NF $\kappa$ B (Supplementary

Figure 3). Secretion and maturation of IL1 $\beta$  depends on inflammasome activation and caspase-1.<sup>19,28</sup> Immunohistochemistry of caspase-1 shows expression within infiltrating inflammatory cells but not in pancreatic acini 3 days after duct ligation (Figure 6B). Secretion of mature IL1 $\beta$  from macrophages in response to acini proves in vitro activation of the inflammasome; in contrast, CCK-stimulated acini did not secrete IL1 $\beta$ . Blockade of macrophage cathepsins by CA074me or E64d abolished IL1 $\beta$  secretion (Figure 6C). Genetic deletion of NLRP3, an essential part of the inflammasome complex, did not affect macrophage phagocytosis and intracellular protease activation upon co-incubation with WT acini (Figure 6D). NF $\kappa$ B translocation into the nucleus (Figure 6E), as well as cytokine secretion of IL6, TNF $\alpha$ , and MCP-1, was reduced in the same way as after treatment with nafamostat (Figure 6F).

Protease activation within macrophages results in IL1 $\beta$  maturation and secretion, which enhances the pro-inflammatory macrophage phenotype by acting on the IL1 $\beta$  receptor expressed on macrophages in an autocrine loop (Supplementary Figure 2C).

### Adoptive Transfer of WT Macrophages Restores Trypsinogen Activation During Severe Necrotizing Pancreatitis in CTSB $^{-/-}$ Mice

As previously reported, significant numbers of macrophages migrate into the pancreas during the early phase of pancreatitis, and these infiltrating cells express considerable concentrations of CTSB (Supplementary Figure 4A). In fact, CTSB is the second most abundant protein in macrophages (data not shown). This would make it plausible that macrophages also contribute to intrapancreatic trypsinogen activation in vivo. We therefore induced severe pancreatitis in WT- and cathepsin B-deleted animals. Two days after duct ligation we performed an adoptive transfer of BDMB generated from WT or CTSB $^{-/-}$  mice (Figure 7A) and sacrificed animals 24 hours after adoptive transfer of macrophages. Staining for CTSB indicated the presence of CTSB in all cells of WT animals; however, in WT animals receiving CTSB $^{-/-}$  macrophage transfer, we detected CTSB-negative cells in the pancreas. In contrast, in CTSB $^{-/-}$  mice no signal for CTSB was detected and only CTSB $^{-/-}$  mice that had received WT macrophages displayed some CTSB-positive infiltrating cells in the pancreas (Figure 7B). We

**Figure 4.** BMDM were co-incubated with freshly prepared acini stimulated with 1  $\mu$ mol/L CCK. Co-incubation of macrophages with acini led to intracellular localization of trypsinogen and pancreatic amylase in CD68-positive macrophages (A). Furthermore, co-localization of trypsinogen and CTSB was observed (A). Live-cell imaging with fluorochrome substrates for trypsin (green fluorescent  $\pm$  DAPI [4',6-diamidino-2-phenylindole]) or chymotrypsin (blue fluorescent) demonstrated an intracellular punctiform localization of active pancreatic enzymes within macrophages (B). Western blotting of macrophage lysates stain positive for trypsinogen when co-incubated with acini or trypsinogen, but only macrophages co-incubated with acini showed a band for pancreatic amylase (C). Macrophages from WT animals revealed significantly increased trypsin activity when co-incubated with acini, even with acini of CTSB $^{-/-}$  mice, in contrast to macrophages of CTSB-deleted mice, which showed no increase in trypsin activity if co-incubated with WT or CTSB-deleted acini (D). Inhibition of serine proteases by nafamostat completely abolished trypsin activity. Similarly, inhibition of CTSB activity by CA074me reduced intracellular trypsin activity in macrophages but the uptake of acinar cell proteins, as demonstrated by amylase activity, was not reduced by the nafamostat or CA074me (E). Treatment of macrophages with cytochalasin-B reduced the uptake of acinar cell proteins as well as trypsinogen, resulting in decreased trypsin activity and decreased amylase or chymotrypsin activity in macrophages. CTSB activity was not affected by cytochalasin-B (F). Asterisks (\*) indicate significant differences with  $P < .05$  ( $n = 4-6$ ).

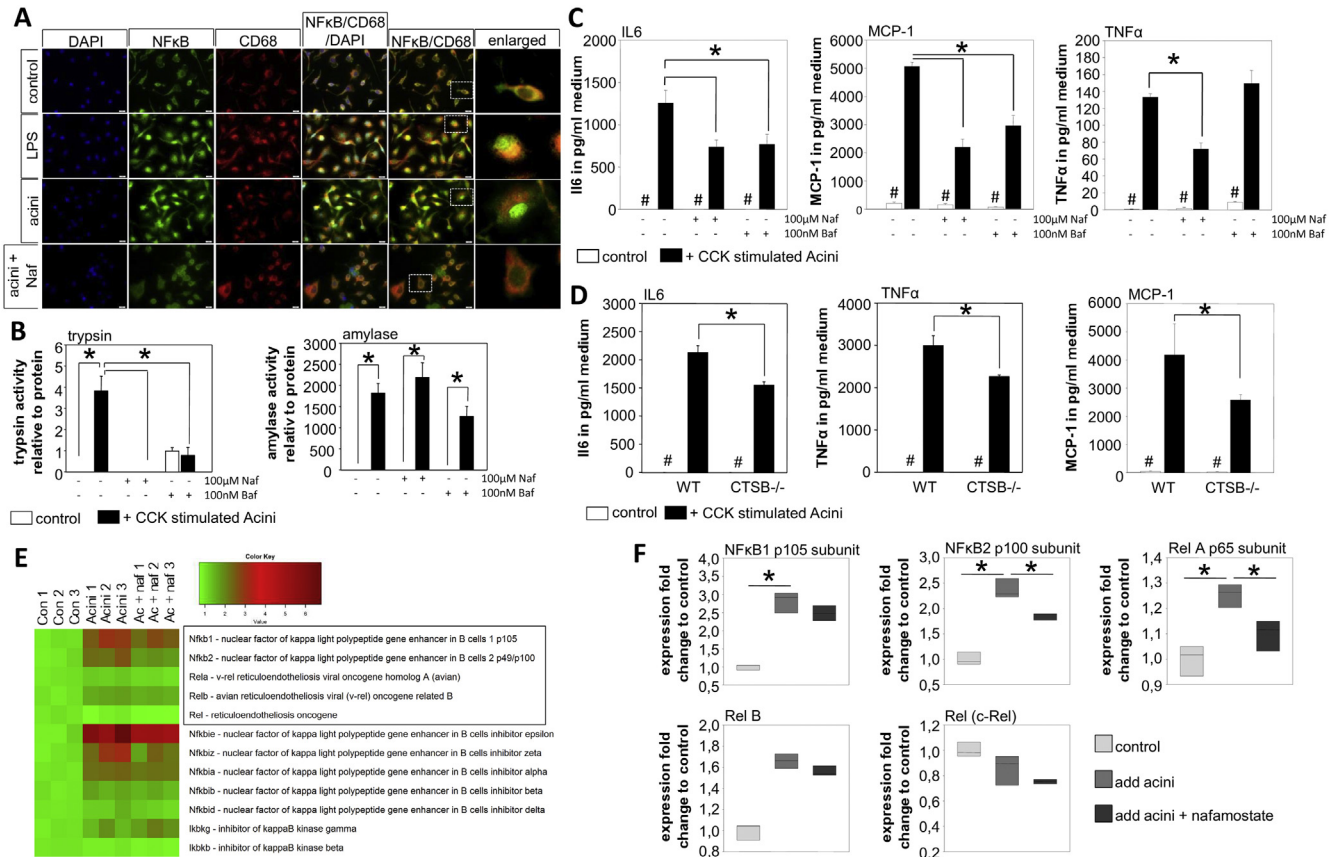


**Figure 5.** BMDM were co-incubated with CCK-stimulated acini for 6 hours. Immunofluorescence staining of NF $\kappa$ Bp65 showed translocation to the nucleus of LPS stimulated macrophages compared with untreated controls. Co-incubation of macrophages and acini resulted in nuclear translocation of NF $\kappa$ Bp65, while treatment with nafamostate prohibited nuclear translocation (A). Treatment with nafamostate as well as bafilomycin-A1 inhibited intracellular trypsin activity in macrophages, but did not affect phagocytosis, as demonstrated by amylase activity (B). After 6 hours of co-incubation, the cytokine release in the supernatant was measured (C). Blockade of protease activation with nafamostate or bafilomycin-A1 significantly reduced IL6-, MCP-1, and TNF $\alpha$  release. The same effect was observed in CTSB-deleted macrophages compared with WT cells (D). Transcriptome analysis showed increased expression of NF $\kappa$ B-related genes in macrophages after co-incubation with acini, which is reduced upon nafamostate treatment for *Nfkb2* and *Rela* (E-F). Asterisks (\*) indicate significant differences with  $P < .05$  ( $n = 4-6$ ); # indicate a significant difference of untreated cells compared with treatment.

observed a prominent infiltration of F4/80-positive macrophages in all animals, independently of the adoptive transfer. H&E histology showed pancreatic damage and necrosis in all animals, but to a significantly lesser degree in CTSB-deficient animals (Figure 7B).

CTSB activity in pancreatic homogenates was completely suppressed in CTSB $^{-/-}$  animals and only in animals that had received WT macrophages did we observed an increase in CTSB activity during pancreatitis (Figure 7C). Untreated animals without duct ligation pancreatitis served as control. In pancreatic homogenates from CTSB $^{-/-}$  mice, we detected only traces of active trypsin and even after induction of pancreatitis we did not detect a significant increase in trypsin activity when CTSB $^{-/-}$  macrophages were adoptively transferred. Only in animals that had received WT macrophages we found a significant increase in trypsin activity in pancreatic tissue homogenates (Figure 7C). In line with these results, in CTSB $^{-/-}$  animals adoptive transfer of WT macrophages significantly increased trypsinogen

activation in WT animals compared with mice that had received CTSB $^{-/-}$  macrophages. These data confirm our findings from the in vitro studies that CTSB-containing macrophages contribute to intrapancreatic trypsinogen activation in the course of severe acute pancreatitis in vivo. The time course of trypsinogen activation in the duct ligation model showed elevated trypsin activity over 14 days, and we observed trypsinogen phagocytosing macrophages at all time points (Supplementary Figure 5). Macrophage-derived protease activation depended on the presence of necrosis. A much greater effect on disease severity and systemic inflammation was observed in CTSB $^{-/-}$  animals 3 days after duct ligation (Supplementary Figure 4B and 4C). The differences between CTSB $^{-/-}$  and CTSB $^{+/+}$  animals were more pronounced in the severe model of pancreatitis compared with the mild caerulein-induced disease model.<sup>5</sup> In a genetic model of chronic pancreatitis in *Lamp2*-deficient mice,<sup>29</sup> we observed enlarged CD68-positive macrophages within the pancreas in

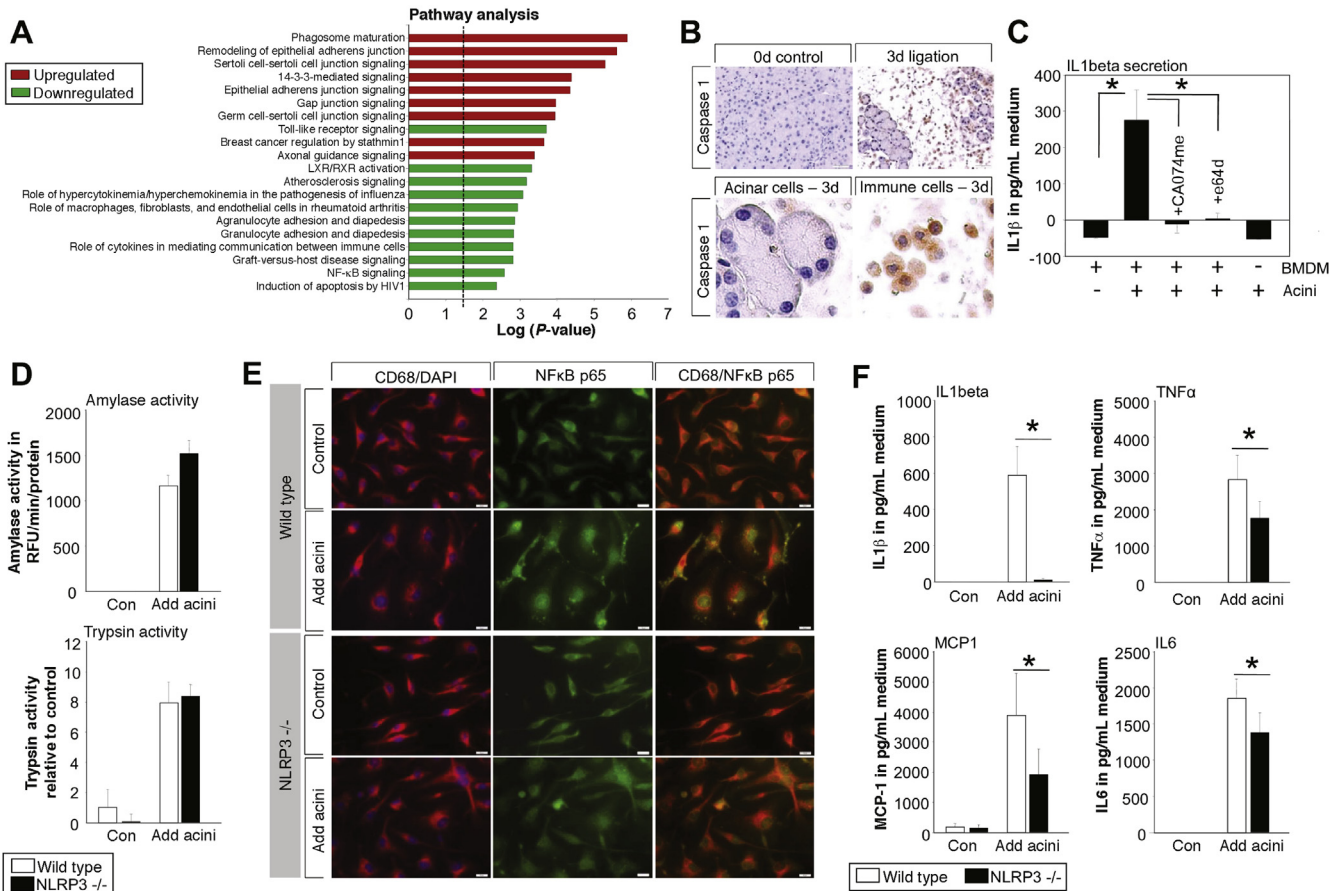


**Figure 6.** Pathway analysis of transcriptome data was performed by using Ingenuity Pathway Analysis software. Major pathways that were induced or repressed in macrophages co-incubated with acini ± nafamostat reveal down-regulation of the toll-like receptor pathway, as well as the NFκB-pathway (A). The major inducer of the NFκB pathway via MyD88 was IL1β.<sup>54</sup> IL-1β maturation depends on caspase-1, which is exclusively expressed in infiltrating inflammatory cells and not in acini during pancreatitis (B). In vitro assay of BMDM revealed secretion of IL1β into the medium 6 hours after co-incubation with acini, while treatment with 50 μmol/L CA074me or 20 μmol/L E64d abolished IL1β release. Acini by themselves were not able to release mature IL1β (C). BMDM from NLRP3<sup>-/-</sup> mice phagocytose in the same way as macrophages from WT mice, as shown by trypsin and amylase content (D). NFκB translocation into the nucleus was reduced in NLRP3-deleted macrophages after co-incubation with acini (E), resulting in a decreased secretion IL6, TNFα, and MCP-1 (F).

conjunction with intracellular trypsinogen and CTSB co-localization (Supplementary Figure 4D).

It is well established that inflammatory response determines the severity of pancreatic damage, and infiltrating monocytes and neutrophils can directly induce acinar cell damage.<sup>10,11</sup> Adoptive transfer of WT macrophages in CTSB-deleted animals resulted not only in an increase in serum amylase but also in serum MCP-1 in animals that had received WT macrophages (Figure 7D). Systemic inflammation thus depends on intra-macrophage trypsinogen activation, which may be the reason why CTSB<sup>-/-</sup> mice display less systemic inflammation.

**Macrophages in Human Pancreatic Tissue**

Paraffin sections of human pancreatic tissue from chronic pancreatitis patients, as well as necrotic tissue from endoscopic necrosectomies, were stained for CD68. Macrophage infiltration was observed in human chronic pancreatitis tissue with regional differences. Tissue samples from

necrosectomy specimens contained only a low number of vital cells, but macrophage infiltration was also observed here (Figure 7E). Co-localization of trypsinogen and CD68 in human chronic pancreatitis samples proved that macrophages phagocytose trypsinogen in humans in the same way as in mouse models of pancreatitis (Figure 7F). In addition to CD68+ macrophages, CD206+ M2 macrophages were also detected in pancreatic tissue, but we never observed co-localization of trypsinogen in CD206+ cells (Supplementary Figure 6). Our data suggest that phagocytosing macrophages can actively contribute to the regulation of the immune response in the course of pancreatitis in mice and men.

**Discussion**

Macrophages are cells of the innate immune system that migrate into the pancreas within hours after the onset of pancreatitis and are involved in local injury via the release of cytokines such as TNFα.<sup>10,30,31</sup> Pancreatitis is primarily a



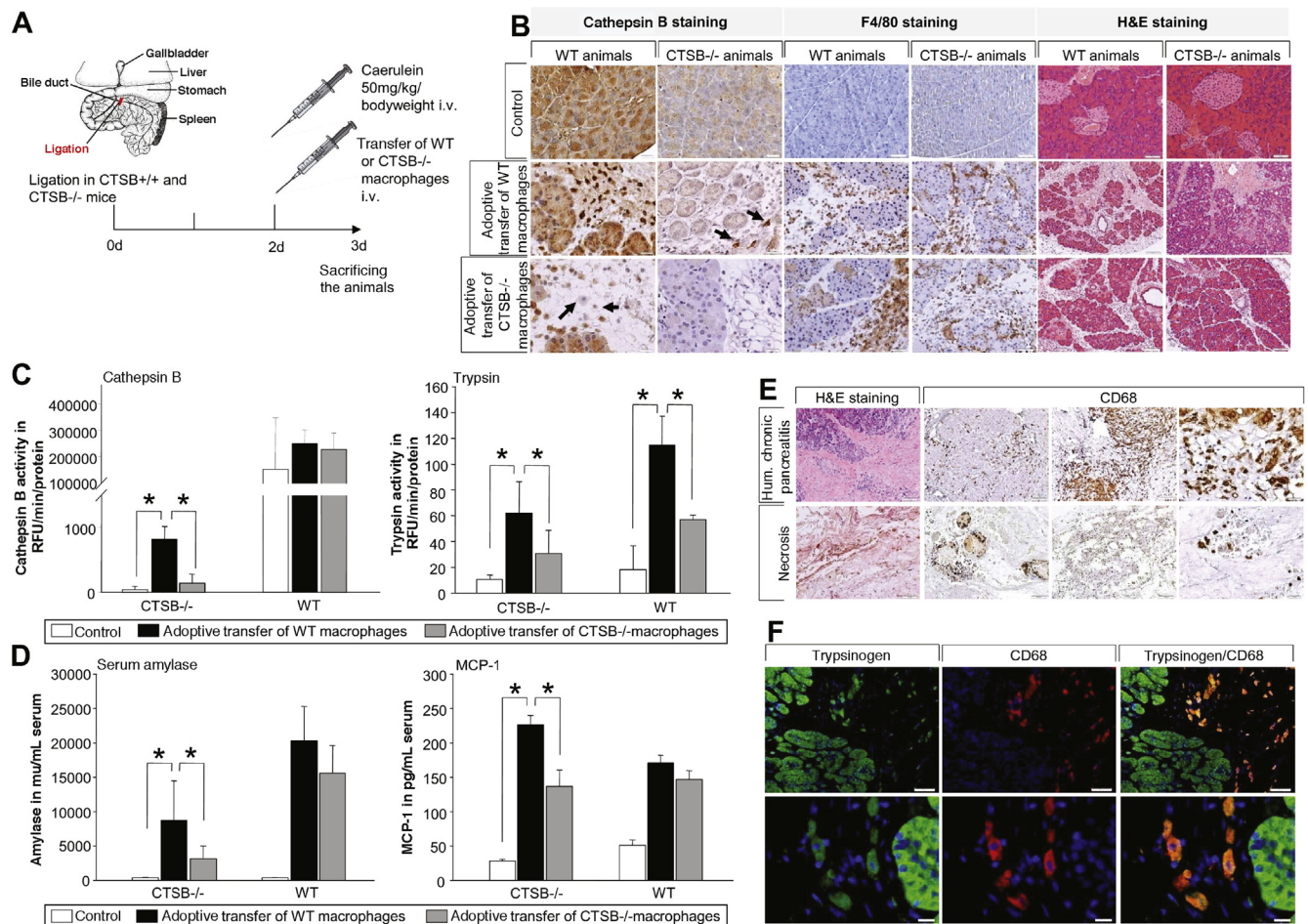


**Figure 7.** Adoptive-transfer of BMDM from WT mice into CTSS-deleted animals and vice versa was performed (A). Staining of CTSS showed infiltrating CTSS-positive cells in the pancreas of CTSS-deleted mice after adoptive transfer of WT macrophages, while adoptive transfer of CTSS-deleted macrophages in CTSS-deleted mice showed no signal (B). F4/80 staining illustrates macrophage infiltration in all animals to the same extent and H&E staining of the pancreas showed pancreatic damage and necrosis in all groups with a higher degree of severity in WT mice (B). Measurement of CTSS activity revealed a significantly higher activity in CTSS-deleted animals treated with WT macrophages, while WT mice displayed the highest activity (C). The adoptive transfer of WT macrophages restored trypsin activity in CTSS-deleted animals, and the additional transfer of WT macrophages in CTSS<sup>+/+</sup> mice resulted in an increase in trypsinogen activation compared with the transfer of CTSS<sup>-/-</sup> macrophages (C). In addition to trypsin activity, serum amylase levels were also increased in CTSS<sup>-/-</sup> animals with CTSS<sup>+/+</sup> macrophages, as well as serum levels of MCP-1 (D). Asterisks (\*) indicate significant differences with  $P < .05$  ( $n = 8-12$ ). Human chronic pancreatitis and necrosectomy specimens were stained for CD68-positive macrophages. Chronic pancreatitis tissue showed in healthy parts a lower number of macrophages and an excessive infiltration of CD68-positive cells in parts of the section where acute damage was observed (E). A human necrosectomy specimen showed only detached areas with CD68-positive cells; for most parts of the tissue only ghosts of cells were detected (E). The highly infiltrated parts of chronic pancreatitis tissue were stained for trypsin and CD68. Here, we detected co-localization of trypsin in CD68-positive macrophages similar to that in mice (F).

sterile inflammation and activation of immune cells in the early disease course is largely independent of infectious pathogens. The activation of immune cells and recruitment of leukocytes is thought to be mediated by the release of pro-inflammatory mediators and chemokines directly from acinar cells<sup>17,30</sup> as well as via DAMPs (eg, free DNA, histones, or free ATP) activating toll-like receptors and the inflammasome complex on immune cells.<sup>19,28</sup> This DAMP-related activation of immune cells links inflammation directly to pancreatic damage. In this context, acinar damage and local inflammation form a causal loop activating each

other in a chain reaction. Intracellular protease activation is known to be a hallmark of pancreatitis<sup>32</sup> but is only indirectly linked to the inflammatory response. From T7 trypsinogen-deleted mice we have learned that NF $\kappa$ B activation can occur independently of trypsinogen activation.<sup>18</sup> So far, most investigations have either focused on acini or on inflammatory cells, while the present project addresses the cross-talk between intracellular protease activation and inflammation.

Macrophages are characterized by a high plasticity. Differentiation of macrophages changes their role in the

pathways of inflammation. Alternatively activated macrophages (M2) have mainly an anti-inflammatory profile promoting wound healing or fibrosis,<sup>33,34</sup> whereas classically activated macrophages (M1) are characterized by a prominent pro-inflammatory phenotype and play a critical role for host defenses against pathogens.<sup>33</sup> In pancreatitis, the role of macrophages appears to change during the different disease stages. In the chronic phase of the disease mainly alternatively activated M2 macrophages are detected in the pancreas and involved in fibrosis formation via stimulation of pancreatic stellate cells.<sup>23,34</sup> In acute pancreatitis, macrophages infiltrate into the pancreas, polarize into the pro-inflammatory M1 phenotype, and drive additional tissue damage.<sup>10,23</sup> Our results show a positive correlation between the extent of pancreatic damage and the number of infiltrating macrophages, whereas for neutrophils no such correlation existed. Because the major task of neutrophils is bacterial clearance by respiratory burst in pancreatitis,<sup>35</sup> a primarily sterile inflammation, the infiltration of neutrophils is more or less an unspecific response, although their ability to form neutrophil extracellular traps within small pancreatic ducts appears to contribute to disease progression.<sup>36</sup> In contrast to neutrophils, monocytes and macrophages can fulfill multiple functions depending on their polarization.<sup>33</sup> One of these functions is the elimination of apoptotic cells, necrotic tissue, and cellular debris.<sup>20</sup> Removal of apoptotic or necrotic cells is a crucial function of macrophages and necessary for maintaining tissue homeostasis and regeneration.<sup>37</sup> We could show that CD68-positive macrophages are attracted to necrotic areas in the pancreas where they phagocytose cellular debris. Cells that undergo apoptosis are rapidly removed without inducing a pro-inflammatory response. Necrotic cell death, the major form of cell death during severe forms of pancreatitis,<sup>38</sup> leads to a pro-inflammatory response of macrophages and can contribute to disease severity.<sup>21,37</sup> We observed a strong pro-inflammatory reaction of macrophages exposed to CCK-stimulated acini, leading to nuclear translocation of NF $\kappa$ Bp65 and the release of high concentrations of pro-inflammatory cytokines. Thus, macrophages trigger a pro-inflammatory reaction during acute pancreatitis. The pro-inflammatory phenotype (M1) depends on necrotic acinar cell death, the lack of DAMP signaling leads to an alternative macrophage activation (M2 phenotype) that is associated with fibrosis induction.<sup>3,4</sup> The balance between M1 and M2 macrophages correlates to the necrosis-fibrosis sequence, which underlines the crucial role of macrophages during acute and chronic pancreatitis.<sup>23,34,39</sup>

The pancreas synthesizes and secretes a multitude of digestive enzymes and, in contrast to other organs, the macrophages of the pancreas could phagocytose large amounts of zymogens when they ingest injured acini or their components. During phagosome maturation, fusion with lysosomes is a critical event for the degradation of phagocytosed content.<sup>40</sup> In pancreatitis, CTSB (the major activator of trypsinogen<sup>5,6</sup>) and pancreatic digestive proteases undergo co-localization within the same

compartment, not only in acinar cells, but apparently also in macrophages. Here we show that trypsinogen undergoes activation in macrophages. This protease activation follows the same pathway as in acinar cells and depends on the presence of CTSB and an acidic pH in the vesicular compartment. Moreover, in mouse models of acute pancreatitis, we could restore protease activation in CTSB-deleted mice by adoptive transfer of CTSB-expressing macrophages and demonstrated their migration into the inflamed pancreas. This means that pancreatic protease activation is not restricted to acinar cells. Protease activation is not only induced in acinar cells by transmigrating leukocytes,<sup>10</sup> it also arises within phagosomes of macrophages. It is well established that the rise in intrapancreatic trypsin activity during pancreatitis follows a biphasic pattern.<sup>5</sup> Intracellular protease activation in acinar cells in the early phase of the disease begins in a zymogen granule-enriched subcellular fraction,<sup>6,32</sup> whereas the second peak of trypsin activity (after hours, rather than minutes) localizes to a lighter, non-zymogen fraction.<sup>6</sup> While it is technically impossible to distinguish the cellular source of trypsin-containing subcellular vesicles, our results make it likely that the second peak of protease activation during pancreatitis originates from macrophages, rather than other types of leukocytes<sup>5</sup> or acinar cells. Prior studies on macrophages during pancreatitis demonstrated a decreased protease activation in mice after macrophage depletion with clodronate-containing liposomes.<sup>10</sup> Severity of disease depends on macrophage-derived cytokine secretion, such as TNF $\alpha$ ,<sup>31</sup> which is responsible for intra-acinar protease activation and necrosis.<sup>10</sup> Our data show that the second, macrophage-driven peak of intrapancreatic trypsin activity has an effect on disease severity. While previous studies have suggested that the initial, intra-acinar cell trypsin activation does not affect the local or systemic inflammatory response,<sup>18</sup> our results indicate that trypsinogen activation within macrophages greatly increases inflammation. The nuclear translocation of NF $\kappa$ Bp65, as well as the pro-inflammatory release of cytokines from macrophages or their differentiation to the M1-phenotype, could be abolished by trypsin inhibition (nafamostat), pH neutralization (bafylomycin-A1), or by deletion or inhibition of CTSB. The regulation of immune responses via serine proteases is not unheard of. During cystic fibrosis, cleavage of the phosphatidylserine receptor by polymorphonuclear leukocyte (PMN) elastase results in impaired macrophage-mediated tissue clearance and ongoing inflammation.<sup>41</sup> *In vitro* experiments using isolated macrophages demonstrated a pro-inflammatory effect of serine proteases that could be prevented by protease inhibitors.<sup>42</sup> Activation of the phosphatidylserine receptor was found to be involved in the anti-inflammatory response of macrophages<sup>43,44</sup> and the recognition of apoptotic cells.<sup>43,45</sup> Another crucial mechanism for macrophage activation is the formation of the inflammasome complex that leads to secretion of IL1 $\beta$ . It is well known that phagosomal rupture and the release of multiple cathepsins into the cytosol induces formation of the inflammasome complex.<sup>46</sup> On the other hand, active trypsin

destabilizes cathepsin-containing compartments like phagolysosomes.<sup>47</sup> Taken together, active trypsin acts as a destabilizing agent on lysosomes that induces inflammasome activation and IL1 $\beta$  release. Macrophages express the IL1 $\beta$  receptor and react in an autocrine pro-inflammatory loop on IL1 $\beta$  stimulation with NF $\kappa$ B translocation to the nucleus.<sup>48</sup> Thus, intra-macrophage protease activation can result in an autocrine loop in macrophage activation that additionally enhances the pro-inflammatory response (Supplementary Figure 7). Even if, according to animal data, blockage of the IL1 $\beta$  pathway could be a therapeutic option for the treatment of severe acute pancreatitis in man, similar to TNF $\alpha$  blockage, we would like to propose a word of caution: It is well known that treating animals with a IL1 receptor agonist (IL1ra) reduces systemic inflammation, and serum levels of IL6 and TNF $\alpha$ , as well as pancreatic damage.<sup>49</sup> Furthermore, genetic deletion of IL1 $\beta$ <sup>50</sup> or components of the inflammasome complex reduce disease severity and systemic inflammation.<sup>19,28,51</sup> However, all those experimental treatments were given prophylactically and we do not have data on the effect of IL1 $\beta$  inhibition in fully established systemic inflammatory response syndrome. Thus, pancreatic inflammation appears to be a self-sustaining mechanism driven by acinar cells and macrophages. Also, in human chronic pancreatitis samples or necrosectomy specimens, macrophage infiltration and ingestion of trypsinogen seem to be a relevant characteristic.

Macrophages appear to play a crucial role in regulating the immune response and are the dominant immune cell population that migrates into the pancreas. In addition, some genetic models of chronic pancreatitis, such as Lamp2-deficient mice or IL1 $\beta$ -transgenic mice, support an important role of macrophages in the disease development.<sup>29,52</sup> Activation and recruitment of macrophages was previously thought to be mediated by cytokine release of acinar cells.<sup>53</sup> Recent data further suggested a critical role of DAMPs, which activate the inflammasome/caspase-1 complex.<sup>19,28</sup> According to our study, a third mechanism of macrophage activation must be added – that induced by intra-macrophage trypsinogen activation. This mechanism is unique to the pancreas, depends on the phagocytosis of cellular components of injured acini in necrotic tissue, depends on the activity of CTSB in macrophages (rather than in acinar cells), and lends itself to therapeutic interventions. Most importantly, targeting intra-macrophage trypsinogen activation would address disease severity at a time point when pancreatitis and tissue necrosis are fully established, rather than trying to treat an early event that most often has already passed when the patient is admitted to the emergency room. This option would clearly be attractive for therapeutic studies.

## Supplementary Material

Note: To access the supplementary material accompanying this article, visit the online version of *Gastroenterology* at [www.gastrojournal.org](http://www.gastrojournal.org), and at <https://doi.org/10.1053/j.gastro.2017.10.018>.

## References

1. Yadav D, Lowenfels AB. The epidemiology of pancreatitis and pancreatic cancer. *Gastroenterology* 2013; 144:1252–1261.
2. Hernández CA, Lerch MM. Sphincter stenosis and gallstone migration through the biliary tract. *Lancet* 1993; 341:1371–1373.
3. Working Group IAP/APA Acute Pancreatitis Guidelines. IAP/APA evidence-based guidelines for the management of acute pancreatitis. *Pancreatol* 2013;13(Suppl 2): e1–e15.
4. Mayerle J, Dummer A, Sendler M, et al. Differential roles of inflammatory cells in pancreatitis. *J Gastroenterol Hepatol* 2012;27(Suppl 2):47–51.
5. Halangk W, Lerch MM, Brandt-Nedelev B, et al. Role of cathepsin B in intracellular trypsinogen activation and the onset of acute pancreatitis. *J Clin Invest* 2000;106: 773–781.
6. Sendler M, Maertin S, John D, et al. Cathepsin B activity initiates apoptosis via digestive protease activation in pancreatic acinar cells and experimental pancreatitis. *J Biol Chem* 2016;291:14717–14731.
7. Hirano T, Saluja A, Ramarao P, et al. Apical secretion of lysosomal enzymes in rabbit pancreas occurs via a secretagogue regulated pathway and is increased after pancreatic duct obstruction. *J Clin Invest* 1991;87: 865–869.
8. Schnekenburger J, Schick V, Krüger B, et al. The calcium binding protein S100A9 is essential for pancreatic leukocyte infiltration and induces disruption of cell-cell contacts. *J Cell Physiol* 2008;216:558–567.
9. Sandoval D, Gukovskaya A, Reavey P, et al. The role of neutrophils and platelet-activating factor in mediating experimental pancreatitis. *Gastroenterology* 1996; 111:1081–1091.
10. Sendler M, Dummer A, Weiss FU, et al. Tumour necrosis factor  $\alpha$  secretion induces protease activation and acinar cell necrosis in acute experimental pancreatitis in mice. *Gut* 2013;62:430–439.
11. Gukovskaya AS, Vaquero E, Zaninovic V, et al. Neutrophils and NADPH oxidase mediate intrapancreatic trypsin activation in murine experimental acute pancreatitis. *Gastroenterology* 2002;122:974–984.
12. Whitcomb DC, Gorry MC, Preston RA, et al. Hereditary pancreatitis is caused by a mutation in the cationic trypsinogen gene. *Nat Genet* 1996;14:141–145.
13. Witt H, Luck W, Hennies HC, et al. Mutations in the gene encoding the serine protease inhibitor, Kazal type 1 are associated with chronic pancreatitis. *Nat Genet* 2000; 25:213–216.
14. Rosendahl J, Witt H, Szmola R, et al. Chymotrypsin C (CTRC) variants that diminish activity or secretion are associated with chronic pancreatitis. *Nat Genet* 2008; 40:78–82.
15. Keim V, Bauer N, Teich N, et al. Clinical characterization of patients with hereditary pancreatitis and mutations in the cationic trypsinogen gene. *Am J Med* 2001;111: 622–626.
16. Whitcomb DC, LaRusch J, Krasinskas AM, et al. Common genetic variants in the CLDN2 and PRSS1-PRSS2



- loci alter risk for alcohol-related and sporadic pancreatitis. *Nat Genet* 2012;44:1349–1354.
17. Gukovsky I, Gukovskaya AS, Blinman TA, et al. Early NF-kappaB activation is associated with hormone-induced pancreatitis. *Am J Physiol* 1998;275:G1402–G1414.
  18. Dawra R, Sah RP, Dudeja V, et al. Intra-acinar trypsinogen activation mediates early stages of pancreatic injury but not inflammation in mice with acute pancreatitis. *Gastroenterology* 2011;141:2210–2217.e2.
  19. Hoque R, Sohail M, Malik A, et al. TLR9 and the NLRP3 inflammasome link acinar cell death with inflammation in acute pancreatitis. *Gastroenterology* 2011;141:358–369.
  20. Poon IKH, Hulett MD, Parish CR. Molecular mechanisms of late apoptotic/necrotic cell clearance. *Cell Death Differ* 2010;17:381–397.
  21. Lawrence T, Willoughby DA, Gilroy DW. Anti-inflammatory lipid mediators and insights into the resolution of inflammation. *Nat Rev Immunol* 2002;2:787–795.
  22. Krüger B, Lerch MM, Tessenow W. Direct detection of premature protease activation in living pancreatic acinar cells. *Lab Invest J Tech Methods Pathol* 1998;78:763–764.
  23. **Sendler M, Beyer G**, Mahajan UM, et al. Complement component 5 mediates development of fibrosis, via activation of stellate cells, in 2 mouse models of chronic pancreatitis. *Gastroenterology* 2015;149:765–776.e10.
  24. Diener MK, Hüttner FJ, Kieser M, et al. Partial pancreatoduodenectomy versus duodenum-preserving pancreatic head resection in chronic pancreatitis: the multicentre, randomised, controlled, double-blind Chro-Pac trial. *Lancet* 2017;390:1027–1037.
  25. **Wartmann T, Mayerle J**, Kähne T, et al. Cathepsin L inactivates human trypsinogen, whereas cathepsin L-deletion reduces the severity of pancreatitis in mice. *Gastroenterology* 2010;138:726–737.
  26. Jungermann J, Lerch MM, Weidenbach H, et al. Disassembly of rat pancreatic acinar cell cytoskeleton during supramaximal secretagogue stimulation. *Am J Physiol* 1995;268:G328–G338.
  27. Bidani A, Heming TA. Effects of bafilomycin A1 on functional capabilities of LPS-activated alveolar macrophages. *J Leukoc Biol* 1995;57:275–281.
  28. Hoque R, Mehal WZ. Inflammasomes in pancreatic physiology and disease. *Am J Physiol Gastrointest Liver Physiol* 2015;308:G643–G651.
  29. **Mareninova OA, Sendler M**, Malla SR, et al. Lysosome associated membrane proteins maintain pancreatic acinar cell homeostasis: LAMP-2 deficient mice develop pancreatitis. *Cell Mol Gastroenterol Hepatol* 2015;1:678–694.
  30. Gukovskaya AS, Gukovsky I, Zaninovic V, et al. Pancreatic acinar cells produce, release, and respond to tumor necrosis factor-alpha. Role in regulating cell death and pancreatitis. *J Clin Invest* 1997;100:1853–1862.
  31. Perides G, Weiss ER, Michael ES, et al. TNF-alpha-dependent regulation of acute pancreatitis severity by Ly-6C(hi) monocytes in mice. *J Biol Chem* 2011;286:13327–13335.
  32. Hofbauer B, Saluja AK, Lerch MM, et al. Intra-acinar cell activation of trypsinogen during caerulein-induced pancreatitis in rats. *Am J Physiol* 1998;275:G352–G362.
  33. Gordon S, Taylor PR. Monocyte and macrophage heterogeneity. *Nat Rev Immunol* 2005;5:953–964.
  34. Xue J, Sharma V, Hsieh MH, et al. Alternatively activated macrophages promote pancreatic fibrosis in chronic pancreatitis. *Nat Commun* 2015;6:7158.
  35. El-Benna J, Hurtado-Nedelec M, Marzaioli V, et al. Priming of the neutrophil respiratory burst: role in host defense and inflammation. *Immunol Rev* 2016;273:180–193.
  36. Leppkes M, Maueröder C, Hirth S, et al. Externalized decondensed neutrophil chromatin occludes pancreatic ducts and drives pancreatitis. *Nat Commun* 2016;7:10973.
  37. Cocco RE, Ucker DS. Distinct modes of macrophage recognition for apoptotic and necrotic cells are not specified exclusively by phosphatidylserine exposure. *Mol Biol Cell* 2001;12:919–930.
  38. Louhimo JM, Steer ML, Perides G. Necroptosis is an important severity determinant and potential therapeutic target in experimental severe pancreatitis. *Cell Mol Gastroenterol Hepatol* 2016;2:519–535.
  39. Gea-Sorlí S, Closa D. Role of macrophages in the progression of acute pancreatitis. *World J Gastrointest Pharmacol Ther* 2010;1:107–111.
  40. Levin R, Grinstein S, Canton J. The life cycle of phagosomes: formation, maturation, and resolution. *Immunol Rev* 2016;273:156–179.
  41. Vandivier RW, Fadok VA, Hoffmann PR, et al. Elastase-mediated phosphatidylserine receptor cleavage impairs apoptotic cell clearance in cystic fibrosis and bronchiectasis. *J Clin Invest* 2002;109:661–670.
  42. Fadok VA, Bratton DL, Guthrie L, et al. Differential effects of apoptotic versus lysed cells on macrophage production of cytokines: role of proteases. *J Immunol* 2001;166:6847–6854.
  43. Huynh M-LN, Fadok VA, Henson PM. Phosphatidylserine-dependent ingestion of apoptotic cells promotes TGF-beta1 secretion and the resolution of inflammation. *J Clin Invest* 2002;109:41–50.
  44. Hoffmann PR, Kench JA, Vondracek A, et al. Interaction between phosphatidylserine and the phosphatidylserine receptor inhibits immune responses in vivo. *J Immunol* 2005;174:1393–1404.
  45. Fadok VA, Bratton DL, Rose DM, et al. A receptor for phosphatidylserine-specific clearance of apoptotic cells. *Nature* 2000;405:85–90.
  46. Orłowski GM, Colbert JD, Sharma S, et al. Multiple cathepsins promote pro-IL-1 $\beta$  synthesis and NLRP3-mediated IL-1 $\beta$  activation. *J Immunol* 2015;195:1685–1697.
  47. **Talukdar R, Sareen A**, Zhu H, et al. Release of cathepsin B in cytosol causes cell death in acute pancreatitis. *Gastroenterology* 2016;151:747–758.e5.
  48. Jung YJ, Isaacs JS, Lee S, et al. IL-1 $\beta$ -mediated up-regulation of HIF-1 $\alpha$  via an NF $\kappa$ B/COX-2 pathway identifies HIF-1 as a critical link between inflammation and oncogenesis. *FASEB J* 2003;17:2115–2117.

49. Norman J, Franz M, Messina J, et al. Interleukin-1 receptor antagonist decreases severity of experimental acute pancreatitis. *Surgery* 1995;117:648–655.
50. Denham W, Yang J, Fink G, et al. Gene targeting demonstrates additive detrimental effects of interleukin 1 and tumor necrosis factor during pancreatitis. *Gastroenterology* 1997;113:1741–1746.
51. Hoque R, Farooq A, Ghani A, et al. Lactate reduces liver and pancreatic injury in Toll-like receptor- and inflammasome-mediated inflammation via GPR81-mediated suppression of innate immunity. *Gastroenterology* 2014;146:1763–1774.
52. Marrache F, Tu SP, Bhagat G, et al. Overexpression of interleukin-1beta in the murine pancreas results in chronic pancreatitis. *Gastroenterology* 2008;135:1277–1287.
53. Neuhöfer P, Liang S, Einwächter H, et al. Deletion of *I $\kappa$ B $\alpha$*  activates RelA to reduce acute pancreatitis in mice through up-regulation of Spi2A. *Gastroenterology* 2013;144:192–201.
54. Li C, Zienkiewicz J, Hawiger J. Interactive sites in the MyD88 Toll/interleukin (IL) 1 receptor domain responsible for coupling to the IL1beta signaling pathway. *J Biol Chem* 2005;280:26152–26159.

---

Author names in bold designate shared co-first authorship.

Received April 24, 2017. Accepted October 17, 2017.

**Reprint requests**

Address requests for reprints to: Julia Mayerle, MD, Medizinische Klinik und Poliklinik II, Klinikum der LMU München-Grosshadern, Anstalt des öffentlichen Rechts, Marchioninstr. 15, D-81377 München, Germany. e-mail: [julia.mayerle@med.uni-muenchen.de](mailto:julia.mayerle@med.uni-muenchen.de); fax: +49 (0) 89 4400-78887.

**Conflict of interest**

The authors disclose no conflicts.

**Funding**

The Deutsche Forschungsgemeinschaft (DFG MA 4115/1-2/3, DFG SE 2702/2-1, GRK 1947/A3), the Federal Ministry of Education and Research (BMBF GANI-MED 03IS2061A and BMBF 0314107, 01ZZ9603, 01ZZ0103, 01ZZ0403, 03ZIK012), and the European Union (EU-FP-7: EPC-TM), V-630-S-150-2012/132/133 and ESF/14-BM-A55-0045/16.

## Supplementary Materials and Methods

### Acini Preparation

Briefly, cells were maintained and stimulated in Dulbecco's modified Eagle medium containing 10 mmol/L 4-(2-hydroxyethyl)-1-piperazine ethansulfonic acid (HEPES), 2% of bovine serum albumin (BSA) and 1% Penstrep. Stimulation of acinar cells was performed with 0.001 mmol/L CCK over 30 minutes; afterwards, cells were centrifuged for 30 seconds at 500 rpm and resuspended in fresh media to wash out residual CCK.

### Reagents and Antibodies

Macrophage colony stimulating factor (MCSF) was purchased from Miltenyi Biotec. (Auburn, CA). Collagenase of *Clostridium histolyticum* (EC.3.4.24.3) from Serva (lot no. 14007, Heidelberg, Germany) was used for acinar cell isolation. LPS from *Escherichia coli* O26:B6 was obtained from Sigma (St. Louis, MO). Purified enzymes of pancreatic porcine amylase and bovine trypsinogen and caerulein, cholecystokinin (CCK), CA074me, E-64d, and cytochalasin-B from *Drechslera dematoides* were obtained from Sigma (St. Louis, MO). Bafilomycin-A1 was obtained from InvivoGen (San Diego, CA).

Protease activity was measured using the following fluorogenic substrates: trypsin R110-(CBZ-Ile-Pro-Arg)<sub>2</sub> from Invitrogen (Carlsbad, CA), cathepsin B AMC-Arg<sub>2</sub>, cathepsin L R110-(CBZ-Phe-Arg) from Invitrogen, and chymotrypsin Suc-Ala-Ala-Pro-Phe-AMC from Bachem (Bubendorf, Switzerland).

The following antibodies were used: anti-Ly6g (ab25377) from Abcam (Cambridge, UK), anti-CD68 (ABIN181836) from antibodies-online, GmbH (Aachen, Germany), anti-CD206 (OASA05048) from Aviva Systems Biology (San Diego, CA), anti-NF- $\kappa$ B p65 (#8242) from Cell Signaling Technology (Danvers, MA), anti-cathepsin B (AF965) from R&D Systems (Minneapolis, MN), anti-amylase (sc-46657) from Santa Cruz Biotechnology (Dallas, TX), anti-glyceraldehyde-3-phosphate dehydrogenase (clone 6C5) from Meridian (Memphis, TN), anti-chymotrypsin (sc-80750) from Santa Cruz Biotechnology, anti-F4/80 (MCA497R) from AbD Serotec (Raleigh, NC), anti-human CD68 (clone PG-M1) from Dako (Glostrup, Denmark), anti-trypsin (AB1823) from Chemicon International (Temecula, CA), anti-caspase-1(#2225) from Cell Signaling Technology, anti-human CD206 (MAB25341) from R&D Systems, and anti-synollin (ab178415) from Abcam.

### Induction of Pancreatitis in Mice

A mild form of pancreatitis was induced in C57Bl/6 mice by hourly intraperitoneal injections of caerulein (50  $\mu$ g/kg body weight) up to 8 hours.

A second model of severe acute pancreatitis was induced in C57Bl/6 and CTSB<sup>-/-</sup> mice by partial duct ligation of the pancreatic duct with a single additional supramaximal stimulation with caerulein 2 days after ligation, as

previously reported.<sup>1</sup> Animals were sacrificed 3, 7, and 14 days after partial duct ligation. Adoptive transfer experiments were performed 2 days after duct ligation by injection of 2 million cells intravenously; 24 hours after the adoptive transfer animals were sacrificed. Cells for adoptive transfer were isolated from bone marrow as described above and maintained in 10-cm dishes for 5–7 days.

### Tissue Handling

Pancreas was snap frozen in liquid nitrogen and stored at -80°C for enzyme measurement. For histology, tissue was fixed in 4.5% formalin for paraffin embedding or embedded in TissueTec (OCT, Sakura, Los Angeles, CA) for cryo sections. Collected blood samples were centrifuged and serum was stored at -80°C.

### Isolation of BMDM

Femur and tibia of C57Bl/6, CTSB<sup>-/-</sup>, and CTSL<sup>-/-</sup> mice were prepared under sterile conditions. Bone marrow was flushed out of the bones with sterile phosphate-buffered saline (PBS) and passed through a cell strainer (70  $\mu$ mol/L). Cells were washed with sterile PBS, counted, and maintained in 6-well plates or chamber slides for immunofluorescence staining in a concentration of 2.5 million cells/well with RPMI medium (1% Penstrep and 5% fetal calf serum [FCS]). Six hours after isolation from bone marrow medium, non-attaching cells were removed and cells resuspended in fresh medium containing 20  $\mu$ g/ml macrophage colony-stimulating factor (M-CSF). Cells were used 5–7 days after isolation for experiments.

Before stimulation, cells were washed with sterile PBS and medium was replaced by fresh medium. Cells were co-cultured with freshly prepared acinar cells as described before, or with 10  $\mu$ g/ml bovine trypsinogen over 6 hours, untreated cells served as controls. For different experimental settings, 50  $\mu$ mol/L nafamostat, 100 nmol/L bafilomycin A1, 50  $\mu$ mol/L CA074me, or 10  $\mu$ g/ml cytochalasin B were added. Stimulation with 1  $\mu$ g/ml LPS served as positive control for cytokine secretion or NF $\kappa$ Bp65 translocation into the nucleus.

Supernatant was harvested, centrifuged at 10,000 rpm, and frozen at -80°C for cytokine measurement. Cells were washed 3 times with PBS to remove residual acinar cells, cellular waste or remaining bovine trypsinogen and subsequently scraped from the plate in the presence of 100  $\mu$ l PBS. Cell suspension was lysed by ultrasound sonification and stored at -80°C for measurement of protease activity. Samples for Western blotting were lysed in buffer containing 25 mmol/L HEPES, 75 mmol/L NaCl, 0.5% Triton X-100, 5% glycerol, 1 mmol/L EDTA in the presence of 1 mmol/L PMSF (phenylmethylsulfonyl fluoride), 5 mmol/L Na<sub>4</sub>P<sub>2</sub>O<sub>7</sub>, 10 mmol/L NaF (sodium fluoride), and 1  $\mu$ g/ml aprotinin.

### In Vivo Imaging of Proteases in Macrophages

Serum amylase and different protease activities were measured as previously reported using substrates



R110-Ile-Pro-Arg for trypsin, Suc-Ala-Ala-Pro-Phe-AMC for chymotrypsin, R110-Phe-Arg for cathepsin L, and AMC-Arg<sub>2</sub> for cathepsin B. In vivo imaging of active proteases within macrophages was performed in  $\mu$ -dish from Ibidi (Martinsried, Germany). Cells were maintained in  $\mu$ -dishes for 5–7 days in the presence of 20  $\mu$ g/ml MCSF. Co-incubation with freshly prepared acinar cells or bovine trypsinogen was performed over 6 hours; afterwards, cells were washed 3 times with PBS before they were loaded with fluorogen substrates, R110-Ile-Pro-Arg, and/or Suc-Ala-Ala-Pro-Phe-AMC in a concentration of 10  $\mu$ mol/L for 30 minutes. Cells were washed again carefully and maintained in PBS for microscopy.

## FACS Analysis of BMDM

Cells were washed by centrifugation, re-suspended in PBS, and strained through a 40- $\mu$ m strainer. Cells were re-centrifuged and re-suspended in PBS and stained with Zombie-NIR (1:100, BioLegend, San Diego, CA) as a marker for necrotic cells in the dark for 30 minutes at room temperature. After that, cells were washed by centrifugation with FACS buffer (1% FCS in PBS) and then incubated with antibodies for 30 minutes at 4°C. BD Horizon V450-conjugated rat anti-mouse/human CD11b (1:100, BD Biosciences, San Jose, CA) and PE-conjugated rat anti-mouse CD69 (1:100, BioLegend) were used. Cells were washed by centrifugation at +4°C and re-suspended in 200  $\mu$ l FACS buffer to be ready for FACS analysis (Becton Dickinson, Franklin Lakes, NJ). The percentage of activated cells was analyzed by FlowJo (<https://www.flowjo.com/>). CD11b was used as a marker for macrophages, whereas CD69 is an activation marker that is only expressed on activated immune cells.

## Isolation of Zymogen Fraction

Subcellular fractionation of healthy whole pancreas from wild type (WT) mice was performed by sucrose gradient centrifugation in a buffer containing 240 mmol/L sucrose, 5 mmol/L MOPS (3-(N-morpholino)propanesulfonic acid), and 1 mmol/L MgSO<sub>4</sub>, as previously described.<sup>2</sup> Zymogen-enriched fraction was stained with membrane bound red fluorochrome Vybrant CM-Dil cell-labeling solution from Invitrogen.

## Cytokine Measurement in Supernatant

The cytokines IL6 and TNF $\alpha$  and the chemokine MCP-1 in medium were measured by Cytometric Bead Array (CBA) mouse inflammation Kit from Becton Dickinson and Company (BD Bioscience). IL1 $\beta$  in supernatant was determined by Quantikine ELISA from R&D Systems.

## Histology, Immunohistochemistry, and Immunofluorescence

For Masson Goldner staining, a kit from Merck (Darmstadt, Germany) was used. Immunohistochemical staining of F4/80 and cathepsin B as well as CD68 in human chronic pancreatitis and necrosis samples was performed on paraffin sections. For antigen retrieval target, retrieval

solution from Dako was used. Antibodies were used in a dilution of 1:100 in 20% fetal calf serum (FCS) from PAN Biotech (Aidenbach, Germany).

Immunofluorescence stainings were performed from cryo-embedded tissue as previously reported.<sup>3</sup> Anti-CD68 was used as marker for M1 macrophages, anti-CD206 for M2 macrophages, and anti-Ly6g for neutrophils. Quantification of immunologic infiltrate was performed by cell count/field of view. A minimum of 5 pictures/animal was quantified.

Immunofluorescence stainings of BMDM was performed in chamber slides. Cells were maintained as previously described in the presence of 20  $\mu$ g/ml MCSF. Co-incubations with bovine trypsinogen or freshly prepared acinar cells were performed under sterile conditions. Cells were washed carefully after co-incubation with PBS before they were fixed in ice-cold acetone for 30 minutes; 20% FCS was used for blocking as well as for antibody dilution. Incubation with antibodies was performed over night at 4°C; antibodies were used in a dilution of 1:100. Secondary antibody incubation was performed for 1 hour at room temperature. Nuclei were stained by DAPI (1:10,000), slides were mounted with DACO mounting medium for fluorescence slides.

Area quantification of macrophages was performed by the software CellSens Dimensions 1.7.1 from Olympus cooperation (Tokyo, Japan). Quantification of secretory tissue and fibrosis in Masson-Goldner staining was performed by color deconvolution technique using the software ImageJ (Supplement 1).

## Microarray-based Transcriptome Analysis

Microarray-based transcriptome analysis was performed as previously described.<sup>4</sup> Shortly, total RNA was extracted from cells using TRIzol reagent, followed by further column purification and quality control. Individual RNA samples ( $n = 3$ ) were subjected to transcriptome analysis using Affymetrix GeneChip Mouse Gene 2.0 ST Arrays and GeneChip WT PLUS Reagent Kit (Thermo Fisher Scientific Inc., Waltham, MA) according to the manufacturer's instructions. Microarray data analysis was performed using the Rosetta Resolver software system (Rosetta Bio Software, Seattle, WA). Significantly different mRNA levels were defined using the following criteria: one-way ANOVA with Benjamini and Hochberg FDR ( $P \leq .05$ ), signal correction statistics (Ratio Builder software)  $P \leq .05$ , and an expression value ratio between the different conditions  $\geq 1.5$ -fold.

In-silico pathway and functional analysis of differentially expressed genes was carried out using the commercial systems biology-oriented package Ingenuity Pathway Analysis (Ingenuity Systems, Inc. Redwood City, CA).

## Western Blot

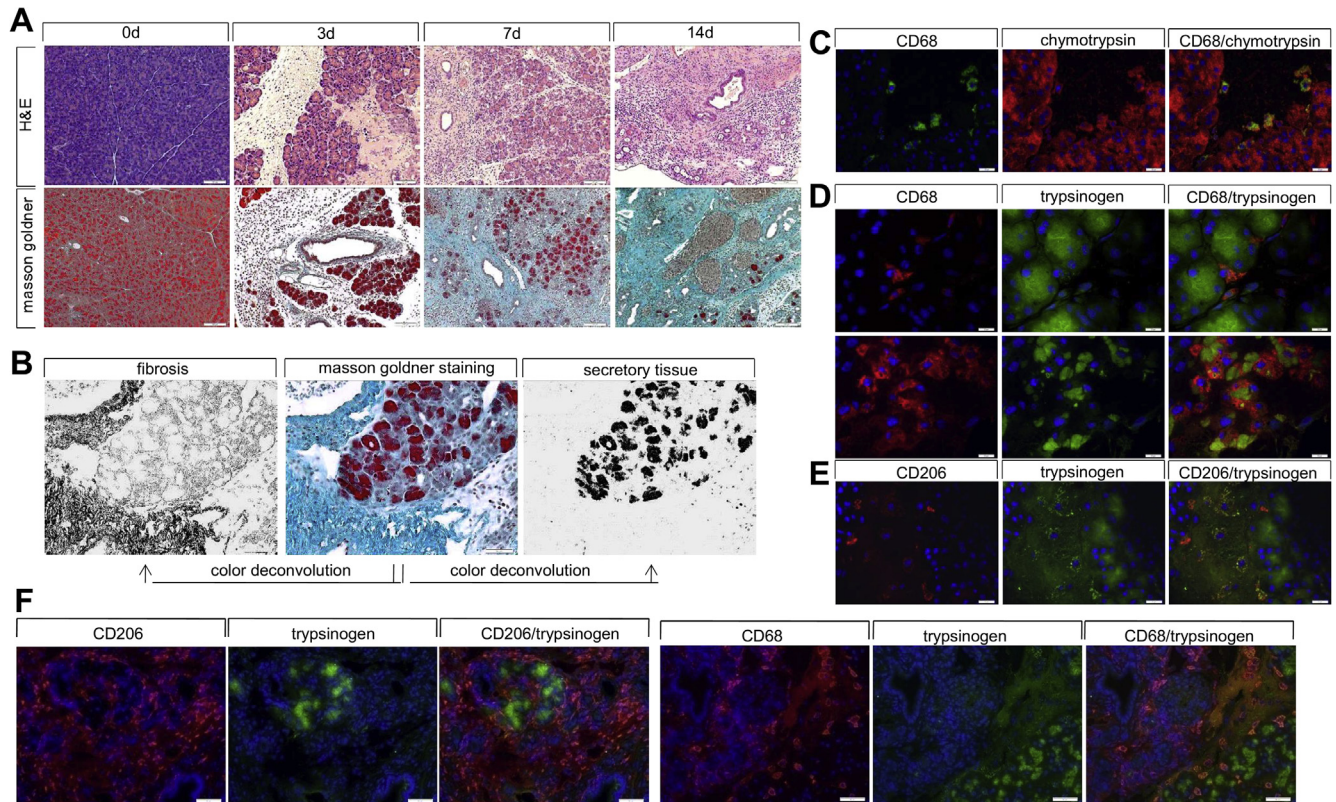
Protein concentrations of samples were determined by Bradford assay; 20  $\mu$ g of total protein was loaded on polyacrylamide gels and transferred onto nitrocellulose for immunoblotting. Anti-amylase, anti-trypsin, and anti-GAPDH antibodies were used in a dilution of 1:1000.

## References

1. **Sendler M, Beyer G**, Mahajan UM, et al. Complement component 5 mediates development of fibrosis, via activation of stellate cells, in 2 mouse models of chronic pancreatitis. *Gastroenterology* 2015;149:765–776.e10.
2. Sendler M, Maertin S, John D, et al. Cathepsin B activity initiates apoptosis via digestive protease activation in pancreatic acinar cells and experimental pancreatitis. *J Biol Chem* 2016;291:14717–14731.
3. Lerch MM, Lutz MP, Weidenbach H, et al. Dissociation and reassembly of adherens junctions during experimental acute pancreatitis. *Gastroenterology* 1997; 113:1355–1366.
4. Lietzow J, Golchert J, Homuth G, et al. 3,5-T2 alters murine genes relevant for xenobiotic, steroid, and thyroid hormone metabolism. *J Mol Endocrinol* 2016;56: 311–323.

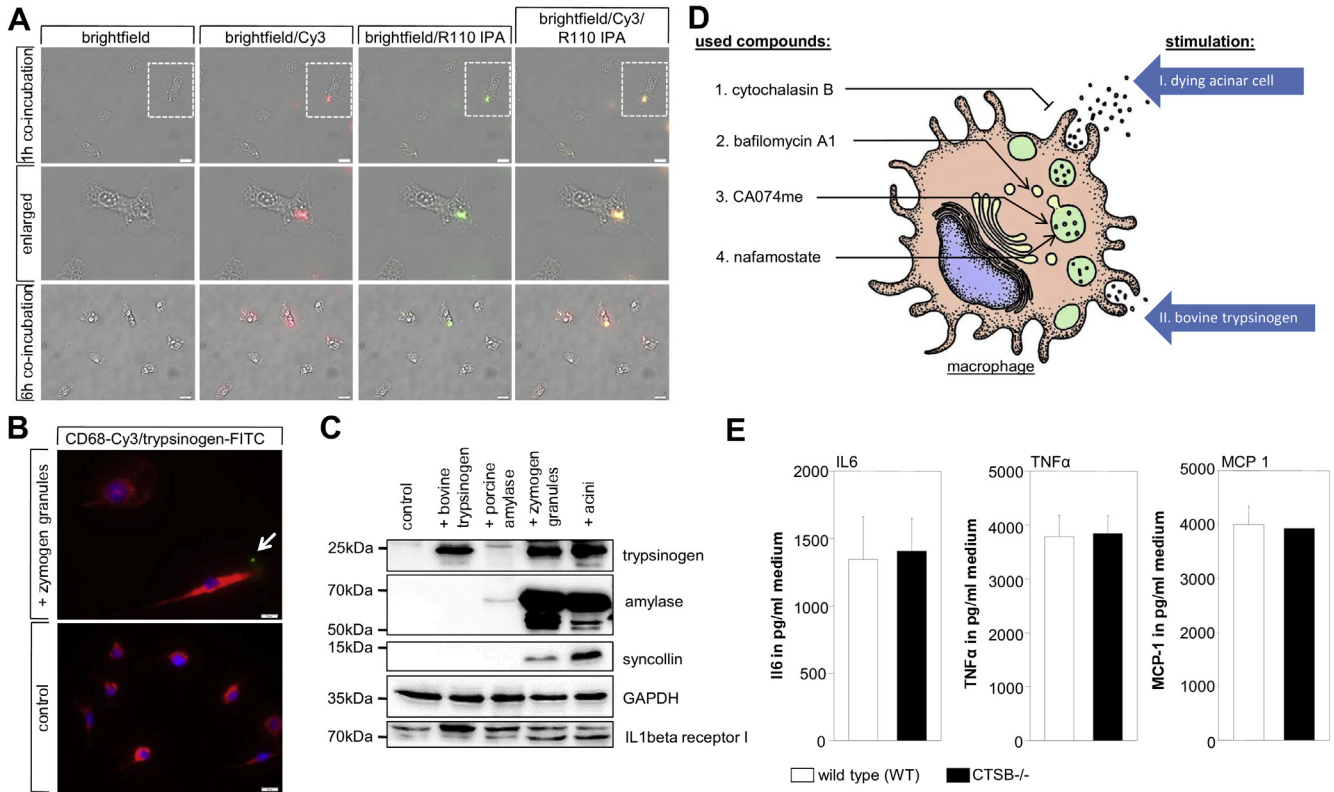
---

Author names in bold designate shared co-first authorship.



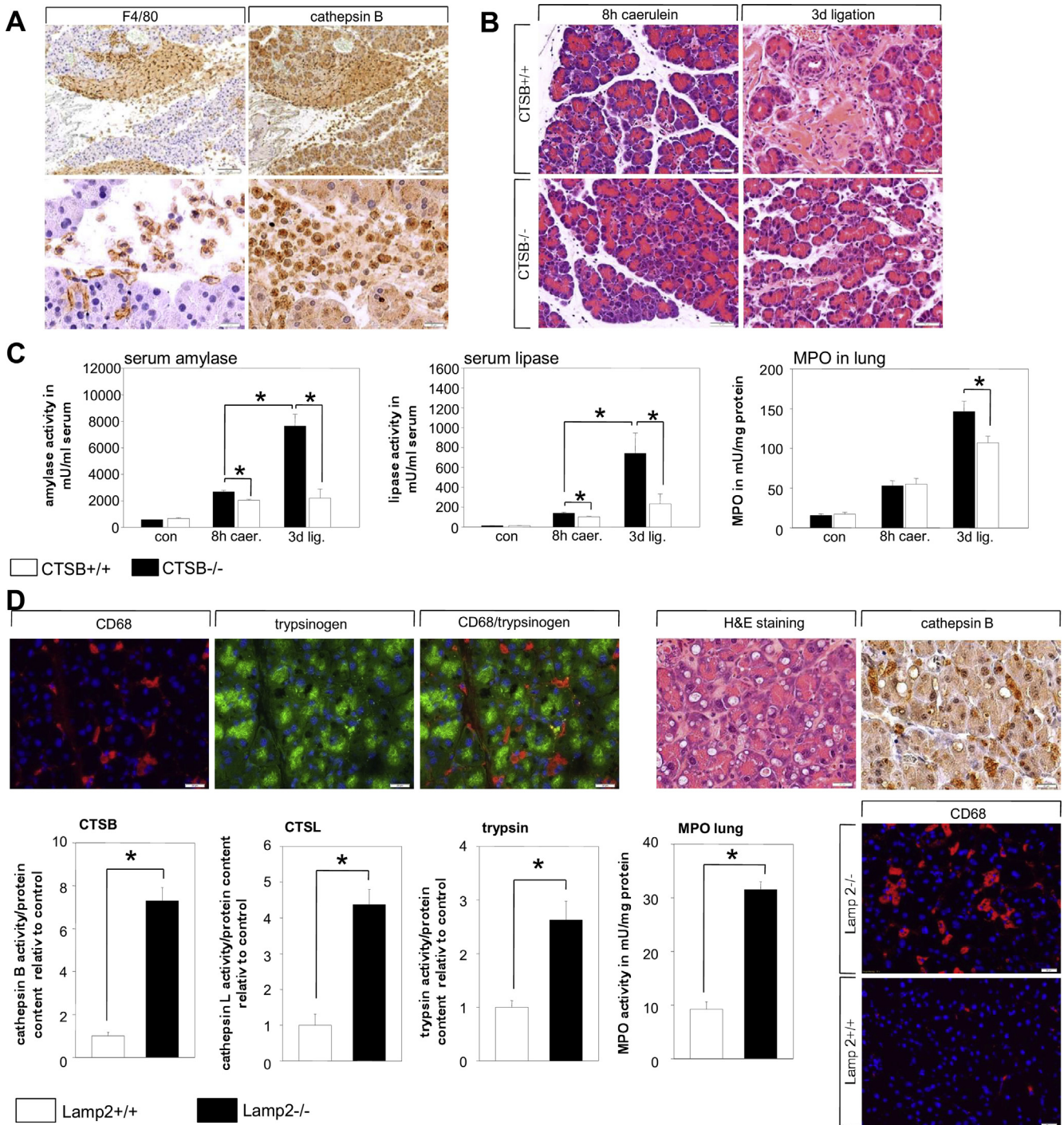
**Supplementary Figure 1.** H&E and Masson-Goldner staining of the pancreas from partial duct ligated C57Bl/6 animals. H&E stainings illustrate necrosis development 3 and 7 days after operation during the severe acute phase of the disease. Masson-Goldner staining revealed development of fibrosis over time, with a maximum at later time points such as day 14 (A). These stainings reflected the necrosis fibrosis sequence in this model. Quantification of fibrosis or healthy exocrine tissue was performed by color deconvolution with ImageJ (B), whereas red areas were regarded as exocrine tissue and green areas as fibrotic tissue. Quantification was calculated in percentage of image taken. Staining of CD68-positive macrophages (Cy3) and trypsinogen (FITC) in pancreas showed intact acini and CD68-positive macrophages without co-localization in necrosis-free areas, but a distinct intracellular localization of trypsinogen in macrophages in necrotic areas (C). Here large amounts of trypsinogen were not associated with DAPI staining and represent extracellular zymogens within necrosis. Co-staining of trypsinogen (FITC) with CD206 (Cy3), a marker for M2 macrophages, in contrast to CD68-positive M1 macrophages (D), showed no co-localization (D). Another pancreatic enzyme, chymotrypsin (Cy3), was also co-localized within CD68-positive macrophages (FITC) (E). Fourteen days after duct ligation we observed an increase of CD206-positive M2 macrophages. These cells do not co-localize with pancreatic trypsinogen (F), but also during this late phase of disease some necrotic areas could be detected where CD68-positive macrophages showed distinct intracellular granules positive for trypsinogen (F).





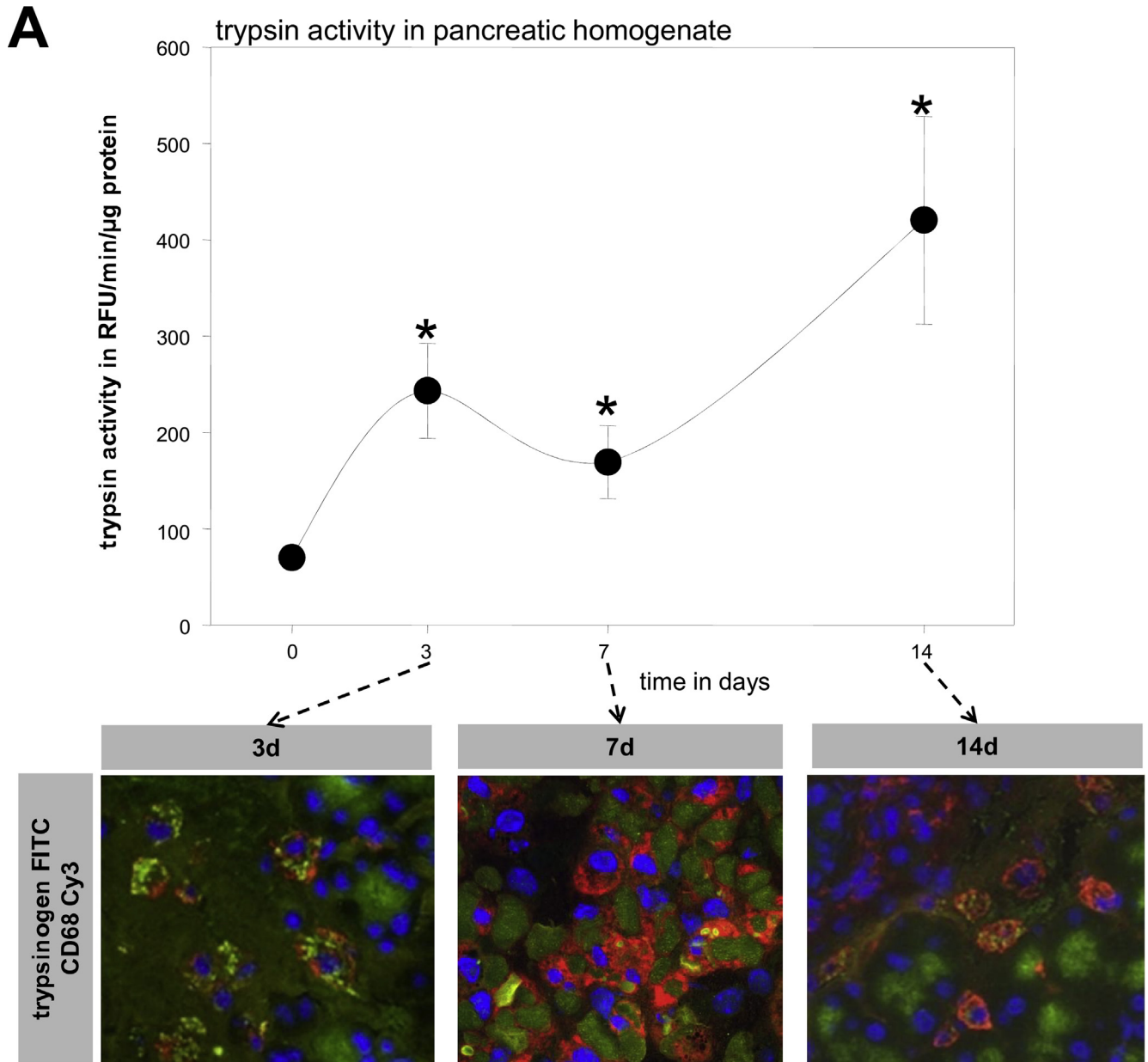
**Supplementary Figure 2.** Co-incubation of BMDM with isolated and fluorescently-labeled zymogen granules revealed an uptake of zymogens by macrophages within 1 hour (A). Loading cells with fluorescent substrate for active trypsin (R110 IPA) demonstrated trypsin activity in phagocytosed zymogen granules. Fluorescent staining of CD68 and trypsinogen showed intracellular localization of trypsinogen in macrophages after co-incubation with isolated zymogen granules (B). Western blot analysis of BMDM confirmed uptake of trypsinogen if macrophages were co-incubated with bovine trypsinogen, zymogen granules, or acini, but not in control cells or cells that were co-incubated with porcine amylase (C). Amylase could only be detected in cells co-incubated with zymogen granules, acini, or purified protein. Syncollin, a zymogen marker, could only be detected in cells co-incubated with zymogen granules or acini. GAPDH served as loading control. The IL1β receptor was expressed independently of co-incubation on macrophages (C). Schematic illustration of experimental set-up for the co-incubation experiments of isolated macrophages (D). BMDM were fed with (I) freshly prepared acinar cell that were stimulated with 0.001 mmol/L CCK before co-incubation, or (II) with 10 μg/ml of bovine trypsinogen. Macrophages phagocytose both dying acinar cells as well as bovine trypsinogen. To investigate the mechanism of macrophage-mediated intracellular protease activation we use different compounds: (1) Cytochalasin B inhibits actin cytoskeleton reorganization and thus prevents phagocytosis; (2) Bafilomycin A1 inhibits V-ATPases and therefore prevents acidification of the lysosomal and phagosomal compartment, which leads to reduced cathepsin B activity; (3) CA074me is a cell-permeable inhibitor of cathepsin B, the major activator of trypsinogen; (4) Nafamostat is a serine protease inhibitor that directly inhibits active trypsin. Stimulation of BMDM from WT and CTSB<sup>-/-</sup> mice with LPS did not show differences in cytokine secretion (E).



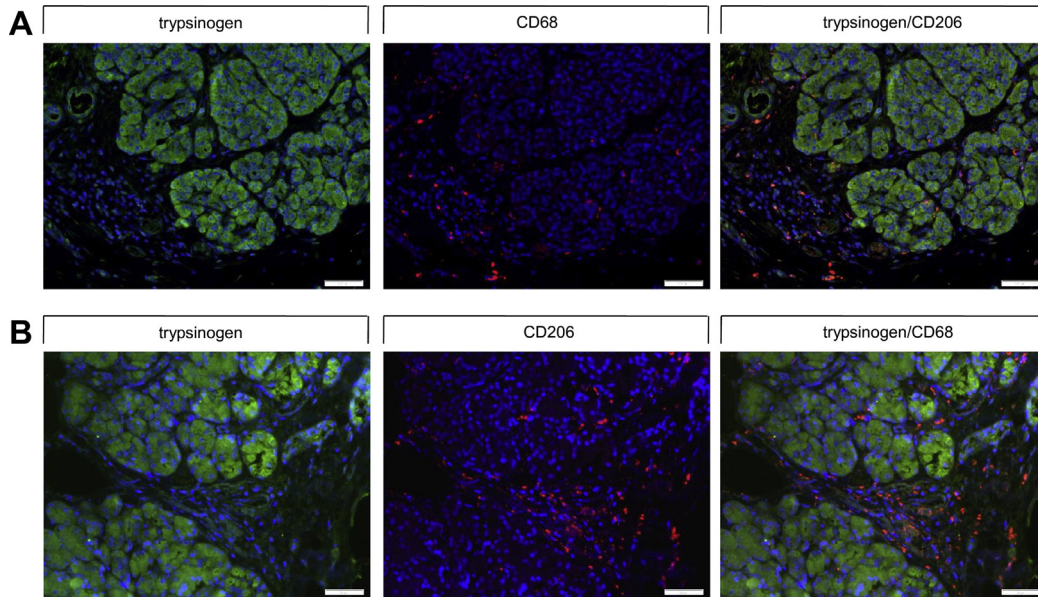


**Supplementary Figure 4.** Macrophages are the dominant infiltrating immune cells during severe necrotizing pancreatitis in mice, demonstrated by F4/80 staining of the pancreas 3 days after duct ligation (A). Staining of cathepsin B illustrates that these infiltrating immune cells carry large amounts of cathepsin B (A). Comparison of caerulein-induced pancreatitis with duct ligation pancreatitis in CTSB<sup>-/-</sup> animals showed slightly decreased pancreatic damage in the model of caerulein pancreatitis and a significant reduction of severity in a severe model of necrotizing pancreatitis (B-C). Serum amylase and lipase were significantly reduced upon duct ligation pancreatitis in CTSB<sup>-/-</sup> mice. In contrast to caerulein-induced pancreatitis, MPO levels in the lung were decreased in CTSB<sup>-/-</sup> 3 days after duct ligation (C). This illustrates the crucial role of CTB mediating the systemic immune response in a severe model of pancreatitis. LAMP2-deficient mice develop chronic pancreatitis spontaneously. In this genetic model of chronic pancreatitis, CD68-positive phagocytosing macrophages co-localized with trypsinogen within the pancreas (D). Staining of CTB shows CTB-positive infiltrating cells within the pancreas. Enzyme measurement of CTB and CTSL demonstrated a significant increase of lysosomal enzymes within the pancreas and trypsinogen activation follows this pattern. LAMP2-deficient mice also showed an increased systemic immune response, illustrated by increased levels of lung MPO. This form of chronic pancreatitis is associated with a strong infiltration of CD68-positive M1 macrophages.



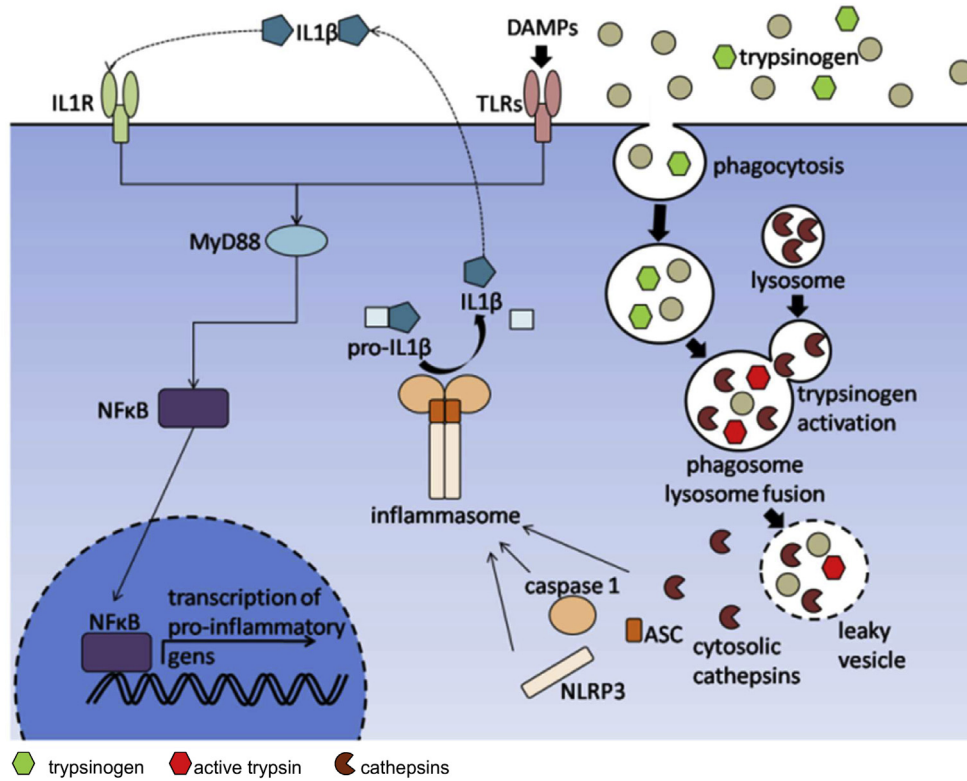


**Supplementary Figure 5.** Trypsin activity was measured over the time course of 14 days after induction of partial duct ligation pancreatitis in pancreatic tissue homogenate. Trypsinogen activation was significantly elevated at all time points (3, 7, and 14 days) compared with untreated control mice (0 days). In addition to the trypsin activity, we observed a co-localization of trypsinogen within CD68-positive macrophages at all time points after induction of pancreatitis.



**Supplementary Figure 6.** Staining of alternatively activated macrophages (M2) by CD206 in human chronic pancreatitis resection specimen and trypsinogen staining excluded co-localization of these proteins. Phagocytosis of zymogens resulted in the differentiation to na M1 phenotype, and thus the surface marker CD206 that is only expressed on M2 macrophages was lost. However, not all M1 macrophages phagocytosed zymogens but expressed CD68, suggesting alternative pathways of activation to be in place (B).

A



**Supplementary Figure 7.**  $\text{NF}\kappa\text{B}$  activation in phagocytosing macrophages depended in part on intracellular protease activation and an autocrine loop via  $\text{IL1}\beta$  receptor signaling. Zymogens that were engulfed by macrophages undergo lysosomal degradation and during this process trypsinogen was co-localized with macrophage-derived cathepsin B in a phagolysosomal compartment. Cathepsin B-mediated activation of trypsinogen led to phagolysosomal leakiness, which resulted in the cytosolic redistribution of cathepsins. Inflammasome activation was induced by cytosolic cathepsin and resulted in the maturation of  $\text{IL1}\beta$  through the proteolytic processing of pro- $\text{IL1}\beta$  by caspase-1.  $\text{IL1}\beta$  is a crucial activator of the  $\text{NF}\kappa\text{B}$  pathway, as suggested by transcriptome analysis (Supplementary Figure 3).